Front. Phys., 2013, 8(4): 412–437
DOI 10.1007/s11467-013-0349-1

REPORT

Introduction to the CDEX experiment

Ke-Jun Kang[1], Jian-Ping Cheng[1], Jin Li[1], Yuan-Jing Li[1], Qian Yue[1], Yang Bai[3], Yong Bi[5], Jian-Ping Chang[4], Nan Chen[1], Ning Chen[1], Qing-Hao Chen[1], Yun-Hua Chen[6], Yo-Chun Chuang[7,*], Zhi Deng[1], Qiang Du[1], Hui Gong[1], Xi-Qing Hao[1], Hong-Jian He[1], Qing-Ju He[1], Xin-Hui Hu[3], Han-Xiong Huang[2], Teng-Rui Huang[7,*], Hao Jiang[1], Hau-Bin Li[7,*], Jian-Min Li[1], Jun Li[4], Xia Li[2], Xin-Ying Li[3], Xue-Qian Li[3,†], Yu-Lan Li[1], Heng-Ye Liao[7,*], Fong-Kay Lin[7,*], Shin-Ted Lin[7,*], Shu-Kui Liu[5], Ya-Bin Liu[1], Lan-Chun Lü[1], Hao Ma[1], Shao-Ji Mao[4], Jian-Qiang Qin[1], Jie Ren[2], Jing Ren[1], Xi-Chao Ruan[2], Man-Bin Shen[6], Man-Bin Shen[6], Lakhwinder Simgh[7,8,*], Manoj Kumar Singh[7,8,*], Arun Kumar Soma[7,8,*], Jian Su[1], Chang-Jian Tang[5], Chao-Hsiung Tseng[7,*], Ji-Min Wang[6], Li Wang[5], Qing Wang[1,‡], Tsz-King Henry Wong[7,*], Xu-Feng Wang[1], Shi-Yong Wu[6], Wei Wu[3], Yu-Cheng Wu[1], Zhong-Zhi Xianyu[1], Hao-Yang Xing[5], Xun-Jie Xu[1], Yin Xu[3], Tao Xue[1], Li-Tao Yang[1], Song-Wei Yang[7,*], Nan Yi[1], Chun-Xu Yu[3], Hao Yu[1], Xun-Zhen Yu[5], Xiong-Hui Zeng[6], Zhi Zeng[1], Lan Zhang[4], Yun-Hua Zhang[6], Ming-Gang Zhao[3], Wei Zhao[1], Su-Ning Zhong[3], Jin Zhou[6], Zu-Ying Zhou[2], Jing-Jun Zhu[5], Wei-Bin Zhu[4], Xue-Zhou Zhu[1], Zhong-Hua Zhu[6]

(CDEX Collaboration)

[1] *Department of Engineering Physics, Tsinghua University, Beijing 100084*
[2] *China Institute of Atomic Energy, Beijing 102413*
[3] *School of Physics, Nankai University, Tianjin 300071*
[4] *NUCTECH Company, Beijing 100084*
[5] *Department of Physics, Sichuan University, Chengdu 610065*
[6] *Yalongjiang Hydropower Development Company, Chengdu 627450*
[7] *Institute of Physics, Academia Sinica, Taipei 11529*
[8] *Department of Physics, Banaras Hindu University, Varanasi 221005*

Corresponding authors. E-mail: †lixq@nankai.edu.cn, ‡wangq@mail.tsinghua.edu.cn

Received March 11, 2013; accepted May 26, 2013

It is believed that weakly interacting massive particles (WIMPs) are candidates for dark matter (DM) in our universe which come from outer space and might interact with the standard model (SM) matter of our detectors on the earth. Many collaborations in the world are carrying out various experiments to directly detect DM particles. China Jinping underground Laboratory (CJPL) is the deepest underground laboratory in the world and provides a very promising environment for DM search. China Dark matter EXperiment (CDEX) is going to directly detect the WIMP flux with high sensitivity in the low WIMP-mass region. Both CJPL and CDEX have achieved a remarkable progress in recent three years. CDEX employs a point-contact germanium (PCGe) semi-conductor detector whose energy threshold is less than 300 eV. In this report we present the measurement results of muon flux, monitoring of radioactivity and radon concentration carried out in CJPL, as well describing the structure and performance of the 1 kg-PCGe detector in CDEX-1 and 10 kg-PCGe detector array in CDEX-10 including the detectors, electronics, shielding and cooling systems. Finally we discuss the physics goals of CDEX-1, CDEX-10 and the future CDEX-1T experiments.

Keywords China Dark matter EXperiment (CDEX), dark matter, poit-contact germanium detector, China Jinping underground Laboratory (CJPL)

PACS numbers 95.35.+d, 95.55.Vj

* Participate as TEXONO members.

Contents

1 Introduction

Observation of the existence of dark matter (DM) undoubtedly was one of the greatest scientific events of the 20th century, then directly searching for DM and identifying it will be the most important and challengeable task of this century.

As a matter of fact, the conjecture about the existence of DM was proposed quite a long time ago in 1933 by Zwicky [1] stating that near the Coma cluster of galaxies velocity distribution implies more cluster mass than luminous matter and then in 1970 and later Rubin [2–4] reported the anomalously rotation curves of galaxies. The astronomical observation shows that the rotational curves of the test galaxies did not obey the gravitational law if only the luminous matter which resided at the center of the cluster existed. Namely, the velocities of test galaxies were supposed to be inversely proportional to the square roots of their distances from the center of the cluster, but instead, the rotational curve turns flat. It implies that there must be some unseen matter in the galaxy, i.e., DM. Moreover, hints about the existence of DM also appear when a collision of two clusters of galaxies was observed [5]. It was observed that for each cluster, the center of mass does not coincide with the center of the luminous matter after a collision between two clusters. It is explained as that two clusters both of which are composed of DM and luminous matter, collide, and after collision, the dark components penetrate through each other because they do not participate in electromagnetic interaction (EM) nor strong interaction, but the luminous fractions of the two clusters interact with each other via EM interaction, so remain near the collision region while the dark parts have left.

Moreover, all astronomical observations indicate that our universe is approximately flat [6], i.e., the total Ω defined as ρ/ρ_c where ρ_c is the critical density and ρ is the total matter density in our universe, is close to unity. However, the cosmic microwave background (CMB) and big bang nucleosynthesis (BBN) data show that the fraction of luminous baryonic matter density Ω_b is less than 5% and over 95% of our universe is dark. Further analysis [7] indicates that DM may take a fraction of 26.7% while dark energy occupies the rest over 68.3%. The dark energy is the most mysterious subject for which so far our understanding about the universe is not enough to give a reasonable answer even though there are many plausible models. By contrary, DM may have a particle correspondence.

The commonly accepted point of view [8] is that the main fraction of DM in our universe is the cold dark matter (CDM), which could be weakly interacting massive

particles (WIMPs) or axions etc. The criteria of being a DM candidate are that the particle does not participate in EM interaction (so it is dark!), namely, it must be neutral (both electric and color) and does not possess inner structure, otherwise it may have intrinsic anomalous magnetic moments and interact with EM field. Thus generally, it is the so-called elementary particle(s). The most favorable candidate of WIMPs is the neutralino in supersymmetry (SUSY) theory [9], even though one cannot exclude other possibilities at the present [10–12]. For example, He *et al.* [13, 14] proposed that a scalar particle darkon can be a possible DM candidate which interacts with detector matter via exchange of Higgs boson. Besides, the technicolor meson [15], asymmetric mirror DM [16, 17], new particles in the little Higgs model [18] as well as many other particles in various models have also been predicted as DM candidates. It is interesting that, thanks to the LHC which has been successfully operating, one may search for such beyond standard model particles at accelerators.

One of the main goals of the detection of DM is to help finding and identifying DM particle(s).

To realize the task, one should design sort of experiments. Detection of DM is by no means a trivial job. It can be classified into the direct and indirect detections. For the first one, we should set an underground detector and try to catch the flux of Galactic DM. It is also supposed that DM particles (WIMPs) weakly interact with the standard model (SM) matter (mainly quarks). However, we really do not have a solid knowledge to guarantee that DM particles indeed weakly interact with the ordinary matter according to the gauge theory. It is just like that a black cat is confined in a dark room where there is no light, and we are required to catch it. Even though the chance of catching it is slim, we still have probability to get it. But if it does not exist in the room, no matter how hard we strive, we can never succeed[1)]. Therefore, generally our project of directly detecting the DM flux is based on such a hypothesis that it does interact with the detector matter via weak interaction.

Another line is the indirect detection of DM. In that scheme, it is hypothesized that DM particle may decay or annihilate into SM particles via scattering among DM particles. The excess of the spectrum of, e.g., $e^{-/+}$ has been theoretically predicted. Some experiments, including AMS-02, have been proposed for observing such predictions and reconstruct properties of DM/WIMPs [19, 20]. In a proposal, the cosmic ray energy spectrum [21] is to be observed by an earth laboratory in China and satellites in the future. The recent results of AMS-02 confirm the e^+ excess which rises from a few GeV to a few hundreds of GeV [22], and a larger energy range will be scanned soon. Whether the excess is indeed a signal of DM is still not answered yet because there exist many other possible sources.

China Dark matter EXperiment (CDEX) is designed to directly detect DM with the highly pure germanium detector, thus later in this work we will concentrate ourselves on the discussion of direct search for DM. Unfortunately, the kinetic energy of DM particle $\frac{1}{2}m\beta^2$ is rather low, generally the fugacity velocity of WIMPs is 200–800 km/s and the value of $\beta = v/c$ is about 10^{-3}, thus for a WIMP particle of 50 GeV, its kinetic energy is only a few tens of keV, which is too small to cause an inelastic transition for the nucleus. When WIMPs hit on the nucleus in the detector material, the impact causes the nucleus to recoil and then the atom would be ionized. When the nucleus is recombined with the electron clouds, photons may be radiated, accompanied by electrical and thermal signals which can be detected by sensitive detectors. Each detector may be designed to be sensitive to one or a few of the signals and then record them which will be analyzed off-line.

Recently, several groups have reported limited success for detecting the DM flux. DAMA [23, 24] reported their observation of the annual modulation signal and then CoGeNT [25] observed several cosmogenic peaks and their results are consistent with the DAMA's. During the first run, the CDMS group [26] observed a few events of dark matter flux and CRESST-II [27] published their observation results. In the world numerous underground laboratories are working hard to search for the signals of DM. Especially, the XENON10 Collaboration [28] reported their result that for spin-independent DM scattering with detector nuclei, cross-sections $\sigma_n > 7\times10^{-42}$ cm^2 are excluded for $m_\chi = 7$ GeV (m_χ is the mass of WIMPs). However, the CDMS Collaboration [29] just reported their new measurements which are in contrary to the XENON10's results, as claimed, the highest likelihood determines that $m_\chi = 8.6$ GeV/c^2 and the cross-section is 1.9×10^{-41} cm^2. To remedy the discrepancy, Frandsen *et al.* [30] have explored possible ways to "ameliorate" the tension and find that light DM scenario can be consistent with both CDMS and XENON10/100. He and Tandean [31] have re-studied the darkon model and found that there exists a ample parameter space in the two-Higgs-doublet model to accommodate the data of both experiments.

Even though it is commonly believed that WIMPs are heavy, neither experiments nor convincing theories definitely rule out the lighter DM candidates of a few GeV or even MeV. The astronomical observation confirms the existence of DM, but we do not know yet its identity and characteristics, namely, if it has a particle corre-

[1)] This is a story presented by Prof. T. Han at a Jinping conference on DM detection, Sichuan, China, 2011.

spondence or is a cosmological defect, what mass(es) it has and how it interacts with SM matter etc. To draw a definite conclusion, precise experimental measurements are necessary. Moreover, considering WIMPs might be light particles, the detections which are sensitive to light DM particles are needed. Such experiments are more difficult than to detect heavy DM particles and set much higher requirements on the detectors.

With its special advantages, such as the thickest rock covering which can shield out most of the cosmic rays and convenient transportation and comfortable working and living condition, China Jinping underground Laboratory (CJPL) would provide an ideal circumstance for DM detection and the new CDEX collaboration has joined the club for direct DM search. The detailed descriptions about the CDEX project will be given in the following sections.

The physics picture of the detection is clear. The detection is proceeded via scattering between WIMPs and nuclei. To extract any information about the fundamental interaction (SUSY, technicolor, darkon or even little Higgs etc.) from the data, much theoretical work and careful analysis must be done. For the theoretical preparation, one has to divide the whole process into three stages. The first is to consider the elementary scattering between WIMPs and quarks or gluons inside the nucleons, from where we need to derive an effective Hamiltonian describing elastic scattering between DM particle and nucleon, then the subsequent stage is the nuclear stage. Since the kinetic energy of WIMPs is rather low and generally the elastic transition dominates, the energy absorbed by the nucleons would eventually pass to the whole nucleus which recoils and is detectable.

The highly pure germanium detector is designed to be sensitive to low energy DM flux.

The interaction can also be categorized into spin-independent (SI) and spin-dependent (SD) ones. So far, the measurements on the SI WIMP-nucleon cross-section can reach an exclusion limit to 10^{-44} cm^2 [32], but for the spin-dependent case, it is only about 10^{-39} cm^2 [33]. It is believed that beyond 10^{-46} cm^2, the cosmic neutrino would compose unavoidable background and the measurements do not make any sense after all.

1.1 Theoretical framework for detection of DM flux

We are dealing with scattering between WIMPs and nucleus, and let us first present the necessary expressions which are related to the detection.

The recoil energy of the nucleus is [16, 17]

$$Q = \frac{|\boldsymbol{q}|^2}{2M} = \frac{1}{2}mv^2\frac{2mM}{(m+M)^2}(1-\cos\theta_{cm}) = \frac{\mu_{red}^2}{M}v^2(1-\cos\theta_{cm}) \quad (1)$$

where m, M stand for the masses of WIMP and nucleus, v is the absolute value of the velocity of WIMP in the laboratory frame, μ_{red} is the reduced mass of WIMP and nucleus, and θ_{cm} is the scattering angle in the center of mass frame of WIMP and nucleus.

WIMP particle interacts with quarks or gluons inside the nucleon [34–37]. Gluons in the hadron do not participate in the weak interaction at the leading order, so that the fundamental processes concern only the interaction between DM particle and quarks.

How to get the effective coupling of $DM--N\bar{N}$ depends on the concrete model adopted in the calculations [36–39].

As noted, if the interaction between the DM particle and quarks is SI, for example the darkon case [13, 14], the particle interaction and the nuclear effect can be factorized and an enhancement factor proportional to A^2 appears.

The observation rates for SI scattering can be written as [9]

$$\frac{\mathrm{d}\sigma}{\mathrm{d}|\boldsymbol{q}|^2} = G_F^2\frac{C}{v^2}F^2(|\boldsymbol{q}|) = \frac{\sigma_0}{4\mu_{red}^2v^2}F^2(|\boldsymbol{q}|) \quad (2)$$

where G_F is the universal Fermi coupling constant, σ_0 is the cross-section at zero-recoil, μ_{red} is the reduced mass of WIMP and nucleus, finally $F(|\boldsymbol{q}|)$ is the nuclear form factor.

For SD elastic scattering with a small momentum transfer, the contribution of the axial vector is dominant

$$g^2l^\mu\bar{q}\gamma_\mu\gamma_5 q \approx g^2\boldsymbol{l}\cdot\bar{q}\boldsymbol{s}q, \quad q = u,d,s \quad (3)$$

where g is the coupling in the concerned theory and l^μ is the leptonic current (could be SI vector and/or SD axial vector). Summing over the contributions of all partonic spin projections, one would step to the interaction between DM particle and nucleon. Thus the effective current for nucleon is [40, 41]

$$\langle p(n)|\sum_{u,d,s} g\bar{q}s_z q|p(n)\rangle \geqslant \sum_{q=u,d,s} A_q^{p(n)}\Delta_q \quad (4)$$

where $\Delta q \equiv s_q(\uparrow) - s_q(\downarrow) + \bar{s}_q(\uparrow) - \bar{s}_q(\downarrow)$, A_q^p and A_q^n can be obtained from the fundamental Hamiltonian [34]. Calculating the SD cross-section is much more complicated than calculating the SI cross-section. For getting more knowledge about the calculation of the cross-sections for SD processes, the readers are recommended to consult the original works [40–43].

1.2 Ultra-low energy threshold experiment

In recent years, an ultra-low energy threshold (ULE) of

about 400 eV has been achieved with the germanium detector based on the point-contact technology, the point-contact germanium (PCGe) detector is used for scanning WIMP of mass as low as 10 GeV. The scientists from Tsinghua University of China first started the experimental preparation in 2003 [44, 45] and ran a first 5 g-mass planar Ge detector for a test. The TEXONO Collaboration runs a 20 g ULE germanium (20 g-ULEGe) detector with the shielding system on the ground near a nuclear power plant in Taiwan and published its physics results in 2009 shown in Fig. 1 [46]. The CoGeNT Collaboration has also started a similar experiment for WIMP search with PCGe detectors at underground laboratories from 2006 and published its physics results in 2008 and 2011, respectively [47, 48]. The CoGeNT experiment has explored a low WIMP mass region and its results are shown in Fig. 2.

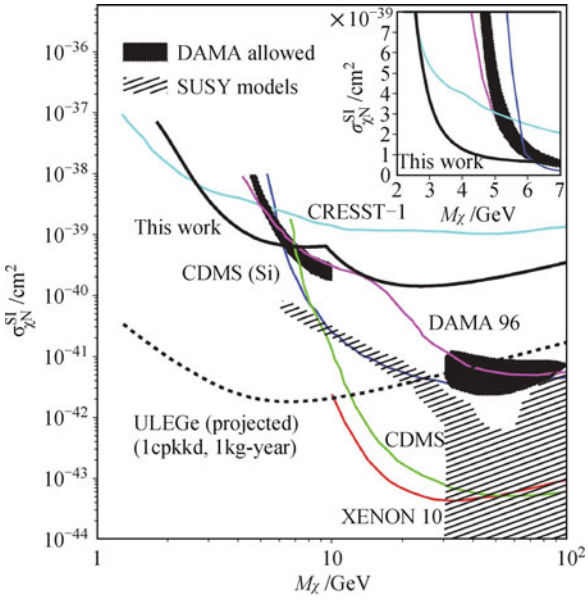

Fig. 1 The physics results of WIMP detection from TEXONO Collaboration [46].

Due to the updated results from Ge detectors, the low-mass WIMP detection has become one of the new hot topics for DM experiments. Many groups have tried to develop lower threshold detectors to scan the low mass WIMP region below 10 GeV. The Majorana [49] and GERDA [50] groups try to reduce their energy threshold to cover the energy range for both double beta decay and DM search.

Since 2009, the CDEX Collaboration has been aiming to search for low mass WIMPs with a ton-scale PCGe detector located at CJPL in China. Now the first stage of the CDEX project CDEX-1, where the 20 g-ULEGe detector from TEXONO and a new 1 kg-mass PCGe detector are installed, has already successfully run and begun to take data.

In the following sections we are going to introduce the circumstance of the underground lab, the shielding of cosmic rays neutrons and gammas background, the detectors and electronics, and the measurement methods as well as the preliminary data analysis and concerned Monte Carlo simulation results in some details.

2 China Jinping underground Laboratory (CJPL)

Experiments such as detection on DM, double beta decay and neutrino research in the particle physics domain require ultra-low background laboratories in order to identify the rare events. Those deleterious background events come mainly from the radioactive isotope of environmental materials, high energy cosmic ray muons which originate from the interaction of high energy protons in cosmic rays with atmospheric compounds at outer space, as well as the internal backgrounds from active isotopes in detector materials and the noise of the detector electronics. The ambient radioactive background from the radioactive nuclei could be shielded with efficient shielding system which includes possible passive and active shielding parts. However the high energy muons, which

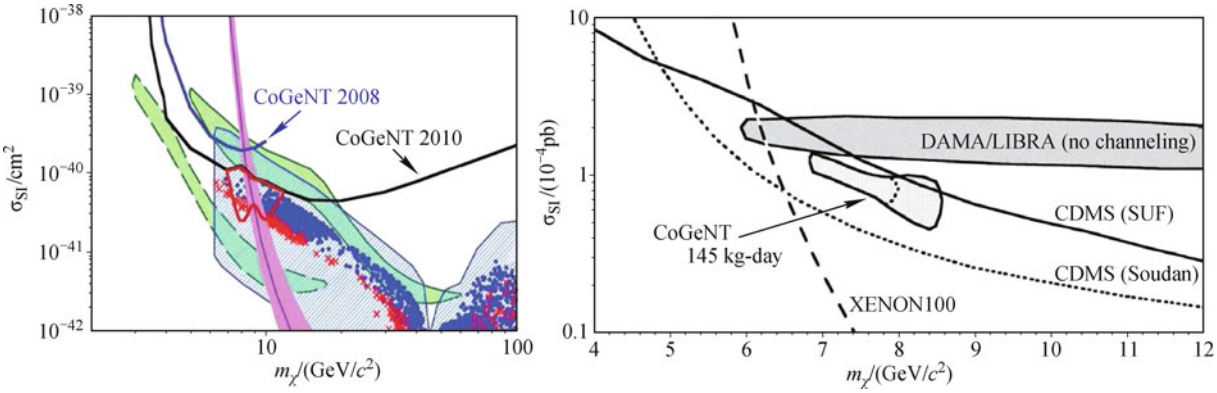

Fig. 2 The physics results of WIMP detection from CoGeNT Collaboration [47, 48].

are the main hard contents of cosmic ray, can pass through the environment and interact with the shielding system materials, the structure materials and the detector itself. Though the instantaneous events coming from direct interaction of muons with those materials on their paths can be vetoed by an active muon veto system, the delayed neutron and accompanying radioactive nuclei induced by incident cosmic ray muons can contribute to backgrounds in the detector. This channel is the most difficult one to be shielded and extracted out from the spectrum of the detection. So it is very necessary that the detection of DM should be performed at underground laboratories where the muon particles are efficiently stopped and absorbed by the overburden rock.

There are many underground laboratories established or under construction in the world including the LNGS in Italy, Kamioka in Japan, Subdury in Canada, Modane in France, Soudan in USA, and so on [51]. In 2010, the deepest underground laboratory was built with excellent working and living conditions in China. This deep underground laboratory is named China Jinping underground Laboratory (CJPL).

2.1 CJPL environment

The Yalong River is more than 1500 km long in Sichuan province of China. A part of almost 150 km of the river bends and encompasses the huge Jinping Mountain to make a narrow arc. The turning is very sharp at the turning point, namely in the mathematical terminology the curvature radius is small at the spot, thus the west and east parts of the river are not much apart, but separated by the mountain and the height difference of their water surfaces is quite large. If a tunnel is drilled from the east to the west along the intercept of the arc, the water drop height is tremendously large, so that this can serve as an ideal hydrodynamic resource. Two hydropower plants at each side of the Jinping Mountain on the Yalong River are being built now by Yalong River Basin (originally called Ertan) Hydropower Development Company. Totally seven parallel tunnels are drilled including one drainage tunnel, two transport tunnels and four headrace tunnels [52]. In 2008, these two transport tunnels were completed and have been in use for the hydropower plant project, and the map is shown in Fig. 3. The length of these two transport tunnels is 17.5 km and the cross-section is about 6 m×6 m. CJPL is located in the central portion of one of the transport tunnels and the rock overburden is about 2400 m thick. Figure 4 shows the detailed location of CJPL in the transport tunnel and the transect profile of the transport tunnel.

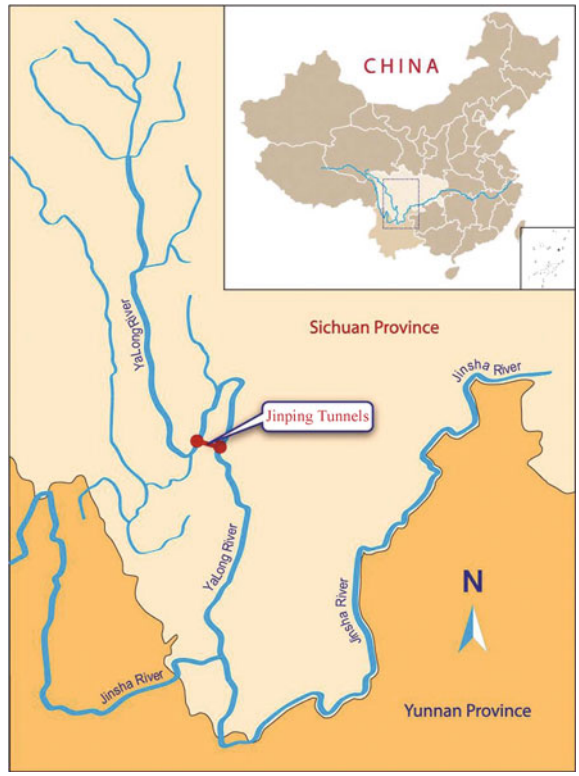

Fig. 3 The site of CJPL.

Tsinghua University, collaborating with Yalong River Basin Hydropower Development Company who owns the Jinping tunnel, had made a plan to build an underground laboratory which was large enough to host a relatively large-scale low-background experiment. The project is under way right now. As the first step, a small CJPL hall has been constructed for DM experiment and an ultra-low background material screening facility has also

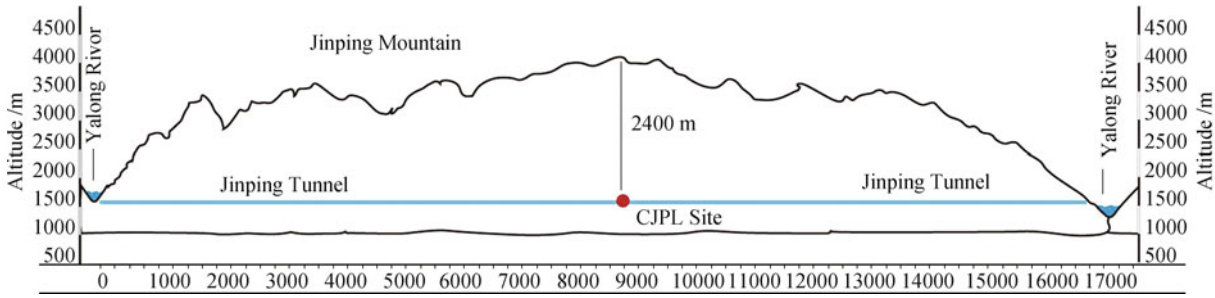

Fig. 4 The cross-section of the Jinping Mountain along the transportation tunnel. The site of CJPL is in the middle part of the Jinping tunnel and can access by drive.

been installed. The CJPL internal space includes three parts: the entrance tunnel of 20 m in length, 30 m long connection tunnel and the main hall with dimension of 7.5 m (H) ×6.5 m (W) ×40 m (L) and the total available volume is about 4000 m^3. The wall of CJPL is covered by a layer of air-proof resin to separate it from the rock of the tunnel. Besides, there are a ground laboratory building, office and dormitory for the researchers near the entrance of the tunnel. Apartments, restaurants, hotel and sport facilities are also available nearby the ground laboratory.

In order to provide a good working condition with fresh air for researchers and further decrease the radon concentration in the air of the internal space, a 10 km long air ventilation pipe has been built to pump the fresh air from outside the transport tunnel into the CJPL space. This ventilation system can provide up to 2000 m^3/h fresh air and keep the air clean inside CJPL. According to the need of DM experiment, the radon trapping system will be installed in CJPL serving as an improved radon gas filter. CJPL is equipped with 3G wireless network and fiber access to broad-band internet.

2.2 CJPL facilities

Low background germanium spectrometer serves as the standard facility for material screening and selection for either detection of DM or neutrinoless double beta decay experiments [53]. The low background germanium spectrometer, called GeTHU facility, with a dedicated low background shield has been designed and set up lately at CJPL for material selection of CDEX and other rare event experiments. Now the facility is operating for background measurement. Moreover, another two counting facilities are being designed to improve minimum detecting sensitivity.

The detector is an N-type, high-purity germanium detector (HPGe) with a relative efficiency of 40% and was constructed by CANBERRA in France [54]. The germanium crystal has a diameter of 59.9 mm and a thickness of 59.8 mm. The cryostat is made of ultra low background aluminum with a U shape to avoid direct line-of-sight to outside [see Fig. 5(a)]. The preamplifier is placed outside the shielding, since it causes more radioactive contaminations.

The shielding structure has been designed to guarantee a large sample space, low background and easy operation. The sample chamber is surrounded by 5 cm (15 cm for the base plate) of oxygen-free high conductivity (OFHC) copper made by the Chinalco Luoyang Copper Co., Ltd. [55]. Three layers of ordinary lead bricks, each 5 cm thick, surround the copper [see Figs. 5(a) and (b)].

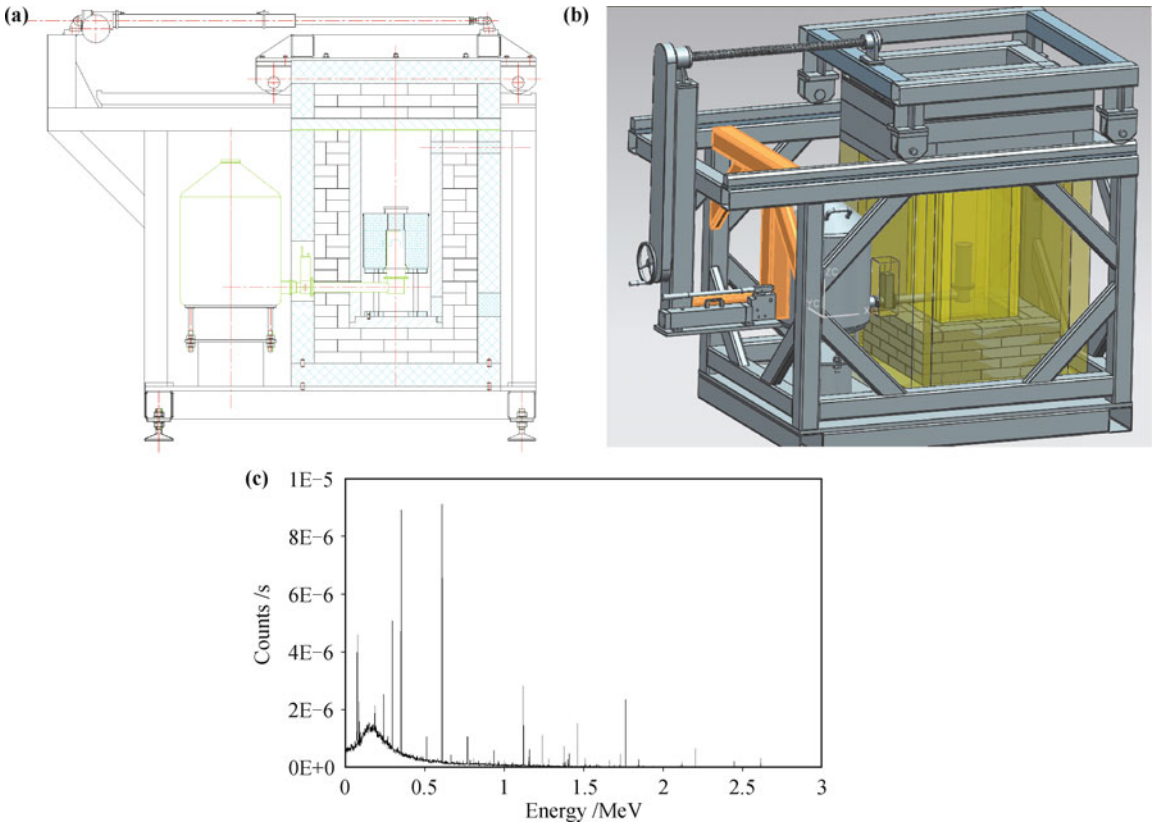

Fig. 5 The ultralow background HPGe gamma spectrometry at CJPL. **(a)** Schematic view of GeTHU at CJPL; **(b)** CAD drawings of GeTHU prototye; **(c)** The background of GeTHU with Monte Carlo simulation.

The ^{210}Pb activity of lead is about 100 Bq/kg. All lead bricks were carefully cleaned by ethanol before installing. Outside the lead are 10 cm borated polyethylene (PE(B)) plates to prevent penetration of ambient neutrons. The upper copper plate, closing the sample chamber, carrying the upper lead bricks and borated polyethylene plates, are placed on sliding rails in order to open or close the shield easily. The whole system is flushed by boiling nitrogen from the cooling dewar. The Monte Carlo simulation shows that the internal background count rate of GeTHU within 40 keV to 2700 keV is only 0.0007 count per second (cps) or so [see Fig. 5(c)].

2.3 CJPL key performance (specification) + simulation

2.3.1 The radioactivity of surrounding environment at CJPL

Original rock samples at different positions in the cave were collected before construction and the concrete samples were collected during the construction. All samples were measured and analyzed by low-background HPGe gamma spectrometer. The measurement results are as follows: the radioactivity concentrations of ^{226}Ra, ^{232}Th and ^{40}K of rock samples are 1.8 ± 0.2 Bq/kg, $<$ 0.27 Bq/kg and $<$ 1.1 Bq/kg; and that of concrete samples are 1629.3 ± 171.3 Bq/kg, 6.5 ± 0.9 Bq/kg and 19.9 ± 3.4 Bq/kg.

Beside the sample measurement, a portable gamma spectroscoper manufactured by ORTEC^{TM} [56] is used to characterize dispersed radioactive nuclides in the environment at CJPL areas. A portable HPGe spectrometer is used to measure the gamma flux at CJPL. The detector consists of a HPGe crystal with a mass of 709 g, the signals from which will be stored and analyzed by the ORTEC^{TM} DigiDART multichannel analyzer (MCA). The spectrometer is set up to measure gamma ray with energies up to 3 MeV and the energy resolution (full width at half maximum, FWHM) is 1.6 keV at 1.33 MeV. Figure 6 shows the in-situ gamma spectrum in different places.

2.3.2 Cosmic ray muon

The main components of cosmic ray which can pass through rock stratum of the mountain are muon and neutrino. The neutrino component can be ignored because of its small interaction cross-section with the detector materials. However, it is very important to know the exact flux of cosmic ray muons for estimating the background event rate caused by cosmic ray directly or indirectly.

In order to obtain the exact value of the muon flux in CJPL, 6 plastic scintillation detectors are employed. The size of plastic scintillators is 1 m$\times$0.5 m$\times$0.05 m. These 6 detectors are divided into groups A and B. The three plastic scintillation detectors of each group are put in erect on a shelf. The up-down distance between neighboring detectors is 0.20 m. The gap between the two groups is about 0.20 m. Schematic diagram of the electronics system is shown in Fig. 7.

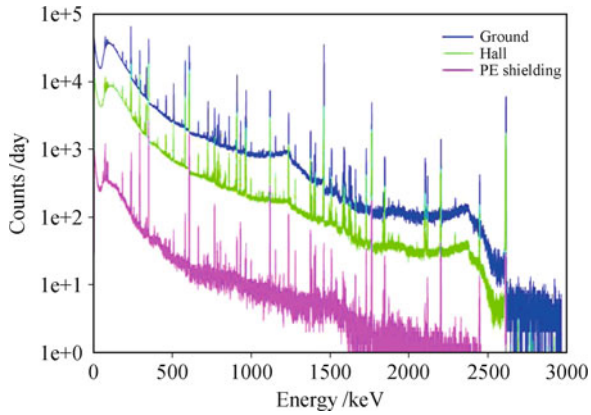

Fig. 6 In-situ gamma spectra in 3 places: CJPL hall (*green line*), CJPL PE shielding room (*purple line*), ground laboratory outside Jinping tunnel (*blue line*).

The performance of the whole detection system was firstly investigated on the ground nearby the entrance of the east end of the tunnel before the measurements inside CJPL. Triple coincidence events of the 3 plastic scintillation detectors in each group is considered as cosmic ray muon events. Because of the large energy deposition of charged muons, signal of muon events are much larger than the noise and signal of ambient gammas.

After the test in ground laboratory, the detection system was moved to CJPL. Based on 171 days' data, the preliminary result [57] is 61.7 ± 11.7 per square meter per year, i.e., about 1 out of 10^8 muons on the ground could survive penetrating into CJPL.

2.3.3 Radon monitoring of CJPL

A decay product of ^{238}U, the noble gas ^{222}Rn as well as its decay daughters, also "observably" contribute to the natural background radioactivity in underground laboratories as it is emanated from the rock and can rather easily enter the detector. Variations of the air radon concentration both in the hall and PE shielding room are continuously measured using two Alphaguard radon monitor manufactured by SAPHYMO GmbH [58] (see Fig. 8). During long period monitoring, the average air radon concentration is $\sim$ 100 Bq/m^3 without ventilation and 50 Bq/m^3 with ventilation.

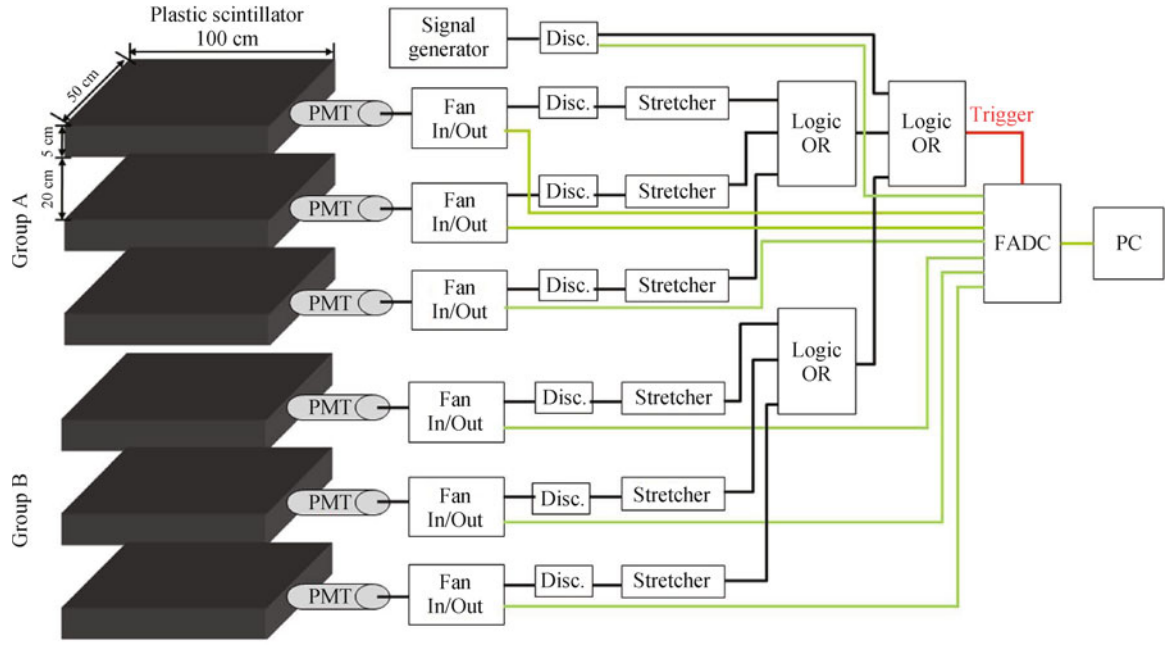

Fig. 7 The electronics system for the cosmic-ray muon veto.

Fig. 8 Radon monitor in CJPL experiment hall.

3 CDEX experiment

3.1 Introduction to CDEX

The main physics goal of the CDEX project is to search for WIMPs in a mass range below 10 GeV with sensitivity better than 10^{-44} cm^2. Because of much more advantages, such as low radioactivity, high energy resolution, high matter density and stability at work, CDEX adopts the PCGe as the target and detector. The recoil energy of Germanium nucleus for low mass WIMPs is only several keV (Fig. 9). Considering the quench factor the threshold of detection should be 100–300 eV for the WIMPs within the range less than 10 GeV. The mass target or detector should be as large as possible because of low event rates. The detector mass of the first phase CEDX-1 is 1 kg and that of the second phase CDEX-10 is 10 kg. The final goal of the CDEX project is to set up to a ton-scale mass Ge detector CDEX-1T in CJPL.

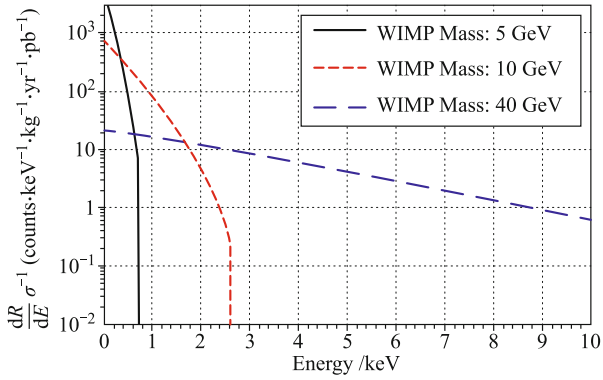

Fig. 9 The recoil energy of PCGe for different WIMP masses.

Obviously, CDEX is a kind of ultra low background experiment. The biggest challenge is to reduce the background event rate to an acceptable level. The expectation of background count level is less than 1 cpkkd. To ensure its successful operation, CDEX must

- hold the detector in CJPL deep underground laboratory;
- establish an efficient shielding system to reduce the background further;
- design a large mass and low threshold detector with tiny amount of internal radioactive isotopes.

As mentioned above, CJPL, which has an overburden of about 2400 m rock, provides an ideal place to host the

CDEX project. In the following, we are going to briefly introduce the detector and the shielding system.

3.1.1 Detector

The physics aim of CDEX composes an unprecedented challenge to the design of the CDEX detector. In summary, the detector should have the following features:

- 1 kg to 1000 kg of detector mass to compensate the extremely low cross-section, namely substantially increase the event rate;
- 200–400 eV threshold. This is because the recoil energies are low, and furthermore only a fraction of these (a low energy quenching factor for Ge recoil of O(20%)) is generally in a detectable form, such as ionization.
- very low concentration of internal radioactive isotopes.

As a semiconductor detector made of the purest material on the earth, the HPGe detector was first proposed to detect WIMP by our group in 2004. By using arrays of commercially available HPGe diodes (5 g, 1 pF capacitance), TEXONO [39] has achieved 220 eV energy threshold. But further increase of the readout channels and monetary investment prevents the detector mass to reach an O(kg) scale.

In order to compromise the mass constraint and energy resolution, small semiconductor detectors usually are the conventional HPGe coaxial detector with low noise and threshold. Instead, CDEX proposes to use PCGe to directly detect the ionization effect of the recoiled Ge nuclei. Figure 10 shows the configurations of coaxial HPGe (*left*) and PCGe (*right*) detectors. By using point contact technology, a PCGe detector can reach an order of 1 kg of mass with very small capacitance (order of 1 pF) and promises intrinsic noise characteristics. Besides the requirements on mass, energy resolution and threshold, it also has the advantages of intrinsic ability to discard multi-site events and surface events. The mass of the detector array can reach a scale up to O(10) kg or even O(1000) kg.

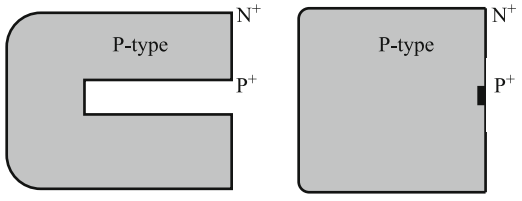

Fig. 10 The configuration of coaxial HPGe (*left*) and PCGe (*right*).

3.1.2 Shielding system

The layout of the CDEX shielding system is shown schematically in Fig. 11. It is located in CJPL, which has a polyethylene (PE) layer with a thickness of 1 m built to decelerate and absorb fast neutrons. Taking into account the commonly accepted WIMP density and elastic scattering cross-sections, the expected event rate is estimated below 0.1 $\mathrm{kg}^{-1} \cdot \mathrm{keV}^{-1} \cdot \mathrm{day}^{-1}$ (cpkkd). These extremely rare events are very difficult to be distinguished from the high backgrounds which come from cosmic rays and natural radioactivity. Then the passive and active shielding systems are proposed (shown in Fig. 12). The outermost layer is a 20 cm lead layer to reduce the environmental gamma ray radiation. The next layer is a 15 cm steel supporting structure. Then, a 20 cm borated polyethylene (PE(B)) layer is used to absorb thermal neutrons. The innermost layer is 10–20 cm OFHC copper for absorbing residual rays. The space inside the copper layer is the room for the HPGe detector and the active shielding system. To reduce the background of radon gas, the inner space of the shielding should be refreshed continuously with highly pure nitrogen gas.

Based on our Monte Carlo simulation of environmental radioactivity and cosmic ray using Geant4 codes as for the environment of CJPL (rocks and concrete): neutrons yielded from the rock and reaching the innermost region of the passive shielding system is 3.129×10^{-12} cpd; the

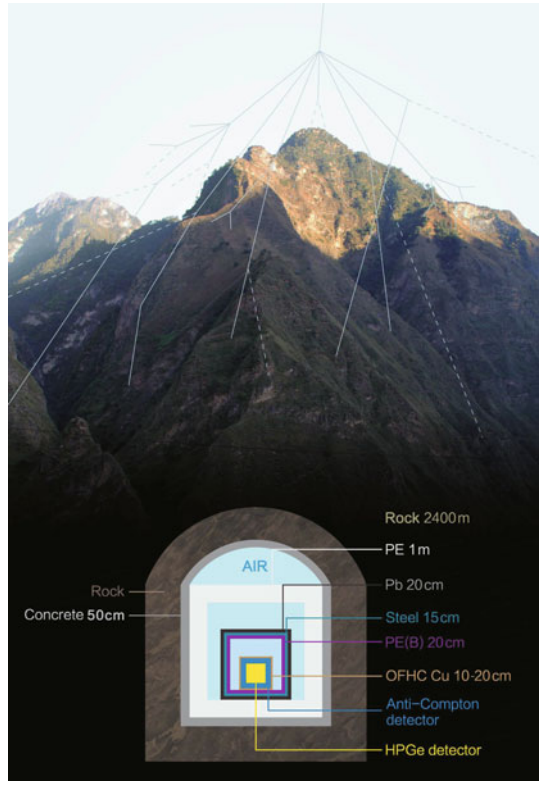

Fig. 11 The layout of CDEX and surrounding rock.

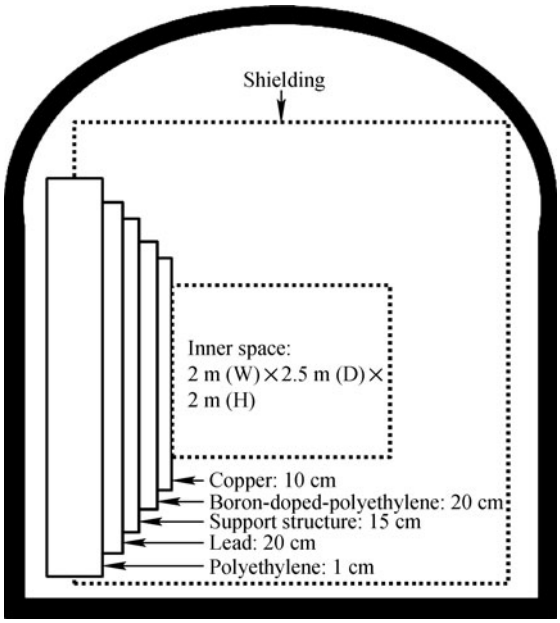

Fig. 12 The schematic diagram of the proposed passive shielding system.

neutrons yielded from the concrete layer and reaching the innermost region of the passive shielding is 6.490×10^{-10} cpd; these two quantities are much smaller than the criteria for neutron background demanded by our expected goal. For the passive shielding system itself: we mainly consider the neutron background yielded from the lead and copper shielding. The unit contents of ^{232}Th and ^{238}U have been simulated, the result is that the neutrons which are produced by 1 ppm of ^{232}Th in lead and finally reach the innermost region of the passive neutron shielding are 3.909×10^{-5} cpd, the neutrons which are produced by 1ppm of ^{238}U and finally reach the innermost region of the passive neutron shielding are 5.848 cpd. The neutrons which are produced by 1 ppb of ^{232}Th in copper and finally reach the innermost region of the passive neutron shielding are 1.480×10^{-4} cpd, the neutrons which are produced by 1 ppm of ^{238}U and finally reach the innermost region of the passive neutron shielding are 2.289 cpd. Thus the neutron background from the environment of CJPL could be reduced very efficiently by the shielding of CDEX. The remaining neutron background mainly comes from the passive shielding system itself. In order to achieve our expected low background, we have to restrict the radioactive content of the copper and lead bricks.

Different active shielding methods are proposed for different phases of the experiments. In the first phase, CDEX-1, CsI(Tl) or NaI(Tl), a veto detector surrounding the HPGe detector is proposed. The Liquid Argon (LAr) veto is proposed in the second phase CDEX-10. In this design, the LAr detector serves as both the passive shielding detector and the low temperature media for the HPGe detector.

3.2 CDEX-1

As the first phase of the CDEX experiment, the detectors with 1 kg mass scale of HPGe, named CDEX-1, have been designed and run first. It includes a ready-made 20 g-ULEGe detector and a 1 kg P-type PCGe (1 kg-PPCGe) detector.

3.2.1 20 g-ULEGe

The 20 g-ULEGe (N-type), manufactured by Canberra in France in 2005, actually consists of 4 duplicate crystal elements. Each 5 g element whose cross-section structure is shown as Fig. 13, has a semi-planar configuration with a P^+ contact on the outer surface, and an N^+ contact of small diameter. Other surface encircling the N+ contact is passivated to suppress the surface dark current. Figure 14 depicts the horizontal cross-section of the cryostat and the positional relationship of the 4 crystals. The cryostat end cap opens a 0.6 mm thick carbon composite window so that an external soft X-ray calibration can be carried out. Near the N^+ contact, a low noise FET is installed which reads the signal and sends it to a pulsed optical feedback preamplifier. Each crystal element has two identical outputs, which are connected to high impedance input of the downstream modules.

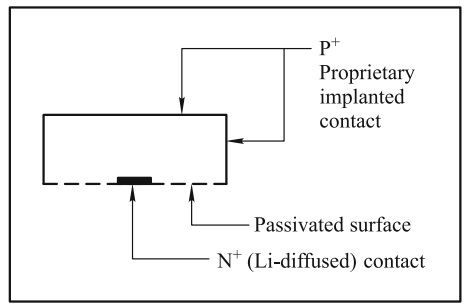

Fig. 13 20 g-ULEGe detector geometry.

Figure 15 simply describes the electronics setup of the 20 g-ULEGe experiment. The output from the preamplifier is directly connected to the conventional spectroscopy amplifier (Canberra 2026), which has high input impedance. The signal is then split: one is input into a FADC (CAEN V1724, 100 MHz sampling frequency) while the other is input into a discriminator to generate trigger control. Meanwhile, random trigger and pulse modules are used to study the efficiency feature etc. The data from the FADC is transferred to PC through a duplex optical fiber.

3.2.2 1 kg-PPCGe

The Germanium detector 1 kg-PPCGe (P-type), manuf-

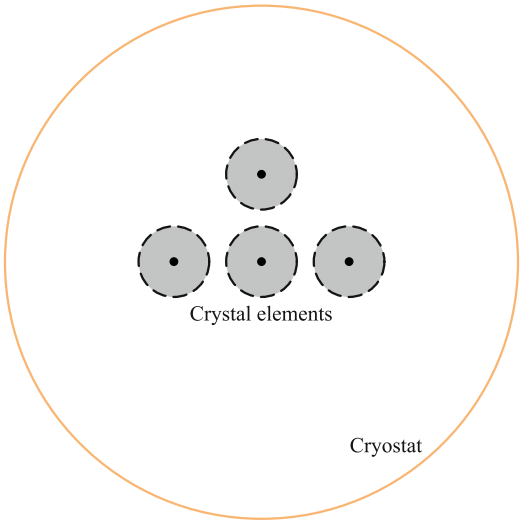

Fig. 14 The horizontal cross-section of cryostat and crystal array.

actured by Canberra in France, was transported to CJPL in 2011. This 1 kg-PPCGe detector, using new point contact technology, has a larger mass: 1 kg (single crystal). The crystal cylinder has an N^+ contact on the outer surface, and a tiny P^+ contact stands as the central electrode. The diameter and depth of the P^+ contact are in order of 1 mm. The small diameter reduces the capacitance (order of 1 pF) of the detector, and readily improves the intrinsic noise standard [59, 60]. The cryostat is designed fully-closed within 1.5 mm thick copper layer, and there is no thin polymer film window.

The 1 kg-PPCGe possesses two preamplifiers, as shown in Fig. 16. The P-type contact signal is read out by a pulsed optical feedback preamplifier, with a low noise EuriFET nearby, while the N-type contact signal is read out by a resistive feedback preamplifier. Both preamplifiers have two identical outputs: OUT T and OUT E.

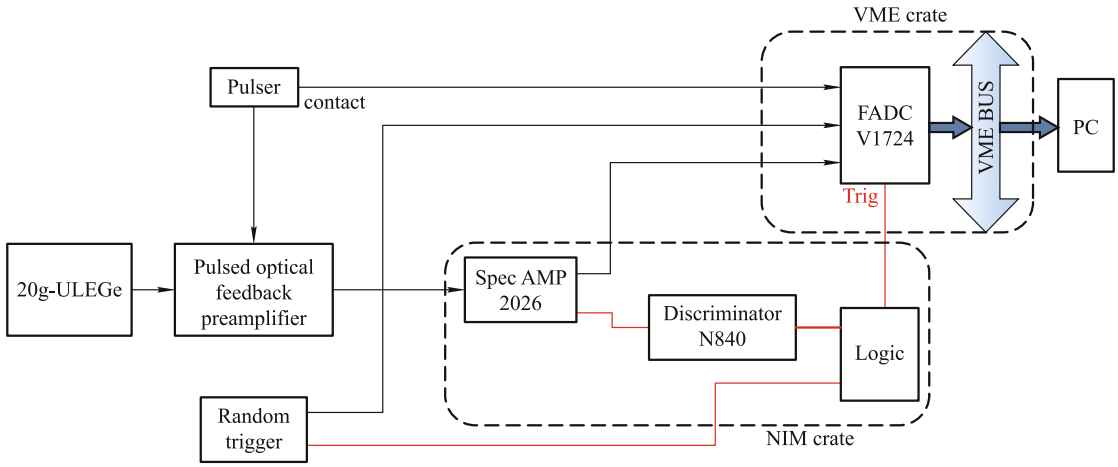

Fig. 15 Simplified schematic diagram of 20 g-ULEGe electronics setup.

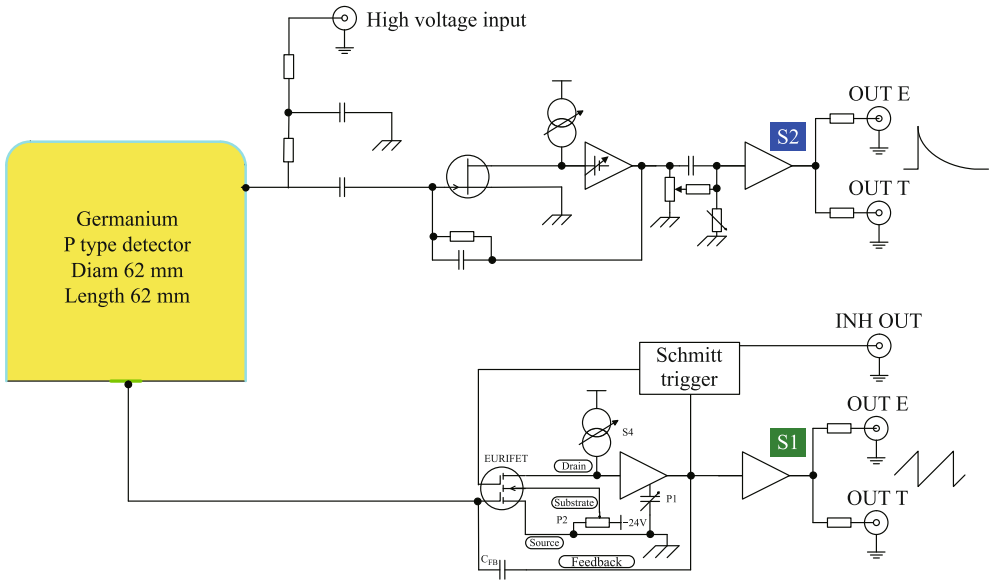

Fig. 16 The front-end electronics of 1 kg-PPCGe in CDEX-1.

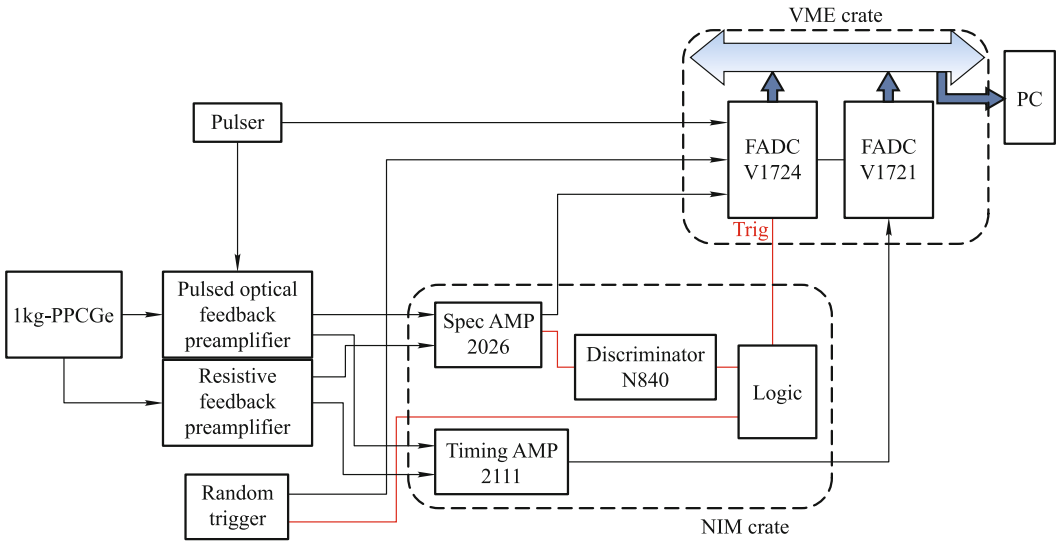

Fig. 17 Simplified schematic diagram of 1 kg-PPCGe electronics setup.

All outputs are connected to the downstream modules which have high input impedance.

For the second phase of CDEX-1 experiment, the electronics set up for running the 1 kg-PPCGe is simply illustrated in Fig. 17. In order to discriminate surface and bulk events, a fast timing amplifier (Canberra 2111) is utilized to amplify the preamplifier signal, and then its signal is injected into a faster FADC (CAEN V1721, 500 MHz sampling frequency). The other preamplifier outputs are directly connected into conventional spectroscopy amplifiers (Canberra 2026), and then fed into the FADC (CAEN V1724, 100 MHz sampling frequency). One signal from P^+ contact is split for trigger control. Again, the random trigger and pulse modules are used to study the efficiency features and etc. The data are transferred into PC through a duplex optical fiber.

3.2.3 Veto detector

The passive shielding system has been well established which can efficiently block the outside gamma ray coming inside, but cannot be 100%. Besides, the shielding materials, even the HPGe detectors, have radioactivity themselves at certain levels. If these rays deposit energy in the HPGe detector, it would be hard to be distinguished from WIMP signals. Luckily, due to the extremely low cross-section of WIMPs scattering with ordinary matter, it is almost impossible that WIMPs can deposit energy both in the HPGe detectors and surrounding materials at the same time. So, the Veto detectors are installed to surround the HPGe detector. By that design, the output signal from HPGe is used as the trigger signal, if there is also signal from surrounding Veto detectors during the same time window, the detected event is not from scattering between WIMPs and detector material and will be filtered. In addition, these Veto detectors are also used for passive shielding. In summary, the Veto detector should have the following features:

- High Z and high density to achieve high veto efficiency and the high shielding ability;
- Low internal radioactivity;
- Low threshold to increase the veto efficiency.

In CDEX-1, CsI(Tl) or NaI(Tl) scintillation detectors are proposed for the Veto detector. Except the features mentioned above, the CsI(Tl) or NaI(Tl) scintillation detectors have the capacity of carrying the pulse shape discrimination (PSD), robust (reasonably soft and malleable, less brittle and less deliquescent for CsI(TI)) and easy to make a large volume. Figure 18 shows the 18 CsI(Tl) crystal array of veto detectors arranged around the cryostat, where each detector is read out by a PMT through a light guide. The advantages of this design are: i) the transportation length of scintillation light is short,

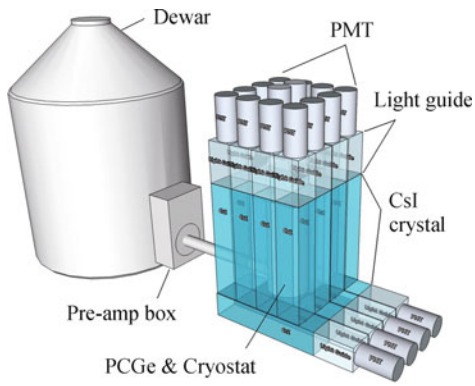

Fig. 18 The schematic diagram of CsI(Tl) veto detector system.

which is good for light collection and lowering the threshold; ii) easy for extension to accommodate larger PCGe detector; iii) the CsI(Tl) crystal bar is easy to produce.

3.3 CDEX-10

Two detectors of CDEX-1, the 20 g-ULEGe and 1 kg-PPCGe, are running at present in CJPL. The data analysis framework has also been set up for the forthcoming data analysis. The CDEX-1 experiment is just the first stage for using low energy threshold Ge detector to directly detect DM. The CDEX-1 experiment will provide more detailed information about the Ge detector performance and the background in the active and passive shielding systems of CDEX in CJPL; at the same time, the preliminary physics results on DM search with these two Ge detectors will be given by the CDEX Collaboration soon.

Synthesizing the recent model-dependent estimation on the cross-sections of scattering between WIMPs and nuclei and the updated results obtained by all the leading underground labs in the world, it is inclined to believe that the detector target mass should be up to ton-scale if the DM experiment tries to "see" the DM, i.e., achieve statistically sufficient event rates with relatively high sensitivity. So the CDEX collaboration plans to directly detect DM with low energy threshold Ge detector of ton-scale target mass. There are several basic conditions which should be considered for the future ton-scale Ge detector. First, the Ge detector module with low energy threshold down to sub-keV scale and enhancing the target mass of the total Ge detector can be done by increasing the number of the Ge detector modules. The second one is that the Ge detector has to include a flexible cooling system to guarantee a low working temperature for the upgrading Ge detectors. The third one is that the Ge detector should possess a veto detector serving as an active shielding against the background contribution coming from the Ge detector itself and the material near the Ge detector.

With this consideration, the whole detector system is composed of two parts: the Ge detector which can be up to ton-scale, is equipped with 1 kg mass PCGe detector modules; another part is the LAr veto detector serving as the cooling system and active shielding. Active shielding system with solid scintillators is abandoned because it is very difficult to enclose large Ge array system, while keeping the Ge detectors being cooled down to the cryogenic temperature. Whereas, LAr could be a good solution. The temperature of LAr is suitable for Ge detector and LAr is also a kind of scintillator which can serve as an active shielding system when the Ge detector is immersed into it.

In order to test the conceptual design of this detector system, learn more details about the technology, and gain experience on both the Ge detectors and LAr veto system, the CDEX Collaboration has designed and will firstly run a 10 kg-scale Ge detectors with LAr cooling and veto system (CDEX-10). The CDEX Collaboration has completed the physics and structure simulation study on the CDEX-10 detector system, and also the conceptual design and related studies on the Ge detectors, LAr cooling system as well as passive shielding system.

The structure of the whole CDEX-10 detector and the shielding system from outside to inside are shown as follows. The interior of a 1 m thick PE room serves as a neutron shielding. This neutron shielding room had been constructed as CJPL was under construction and now we have started to carry out several experiments inside. The second layer is lead shielding against the outside gamma background. The third layer is OFHC copper which shields out the residual gamma background passing through the lead layer and also shields the internal background radiated by the lead shielding. Inside the copper layer there is the LAr veto detector system which serves as both active and passive shielding. As the innermost part, three 0.5 kg or 1 kg PCGe detectors are encapsulated into ultra-pure copper or aluminum tubes which are highly evacuated. One block of the OFHC copper is mounted near the feed through end of the tube to shield the PCGe detector from background produced by the electronics. Several encapsulated tubes with three PCGe detectors are immersed in the LAr vessel for cooling and active shielding. The Total mass of the PCGe detector is about 10 kg. Part of the energy is deposited and the scintillation light is produced when gamma or beta ray enters the LAr. The scintillation light is read out by the photomultiplier tubes (PMTs) and then the signal can serve as a veto signal.

The Ge detector tubes based on the 1 kg-PPCGe detector in CDEX-1 has been manufactured by the Caberra in France according to the CDEX requirement and design. The 1 kg-PPCGe detector for DM search experiment is also the biggest one in the world till now.

In this CDEX-10 detector, the scintillation light is read out by the PMT on the top of the LAr volume. The number of PMT is determined by the detail of the physics design. The design of the cooling and active shielding systems for CDEX-10 LAr has been completed. From the physics point of view, the main requirements for the LAr cooling and active shielding systems are to keep the LAr temperature uniform and stable within a small temperature region to alleviate the temperature dependence of the performances of the PCGe detector, and to prevent the formation of gas bubble and concomitant tiny vibration of LAr which may induce extra noise in the Ge

detector. A number of methods for satisfying such stringent restrictions are considered to maintain constant liquid level and control the generation of gas bubble in LAr under zero boil-off conditions for long periods of time. Large convective motions and pool-boiling are avoided by thermally optimized cryogenic systems to reduce the environmental heat leakage to the low-temperature cryogen, especially, an actively-cooled LAr shield that surrounds the cryostat is used against heat radiation.

3.4 Electronics

The CDEX electronics includes three parts: electronics, trigger system and data acquisition (DAQ) system where:

- The electronics includes the front-end amplifier, the main amplifier, the flash analog-to-digital converter (FADC), as well as high voltage (HV) power supply and the slow-control electronics etc.
- The trigger system contains the trigger system and the clock distribution system.
- The DAQ system contains the data read-out electronics, the slow-control electronics and related data server and memory, communication, display and HMI etc.

3.4.1 Current design of electronics

Considering the future development, a set of multiple-channel electronics for the CDEX detectors has been designed. Figure 19 shows the design architecture of the electronics for our CDEX. The mode is prevailing for both electronics and other parts. So, in the following discussion, a thorough description about the ongoing electronics is made first, and then we will go on describing the next generation of electronics which is under research & development, as well as the concerned engineering problems.

3.4.2 Electronics Architectures of CDEX-1 and CDEX-10

It is forecasted that the signal-readout channels of the larger-scale CDEX detector will be $O(1000)$ in the future. It is necessary to research and develop an electronic system which will be used for both HPGe and veto detectors. The whole electronic system includes the front-end amplifier, main amplifier, FADC and data readout etc. Now the electronic group is focusing their efforts on the design and plan of each parts of the electronic system as described in the following.

- FADC

  According to the physics demand, there are two different kinds of the FADC electronics needed for reading out the pulse shape from the HPGe detector or Veto detector: one is 100 MHz, 14 Bits, 16-channel FADC/GE electronic plug-in with standard dimensions of VME plug-in; another is 1 GHz, 12 Bits, 4-channel FADC/AC electronic plug-in with standard dimensions of VME plug-in. The FADC/GE electronic plug-in is used to read out data on the slow-shaping-time signal of the HPGe, and FADC/AC electronic plug-in is used to read out the fast-shaping-time signal from either HPGe or PMT of the veto detector.

  For convenience and to satisfy different physics demands, the design of the FADC system adopts a new concept which is also being applied in many labs of CERN. The structure uses the same VME board (main board) and different FADC. The experimental facilities are prepared by using different FADC mezzanine cards. Different FADC mezzanine cards are made of FADC chips with different performance indexes and numbers, the channels are connected to the board via the high-speed plug-in. Then the same board is used to conduct data cache, processing and triggering judgment, and then the signals are read out via the standard VME bus

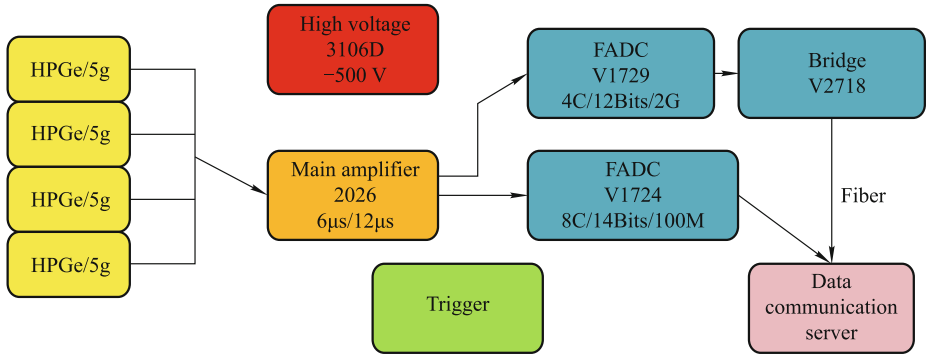

Fig. 19 The ongoing design architecture of electronics: CDEX.

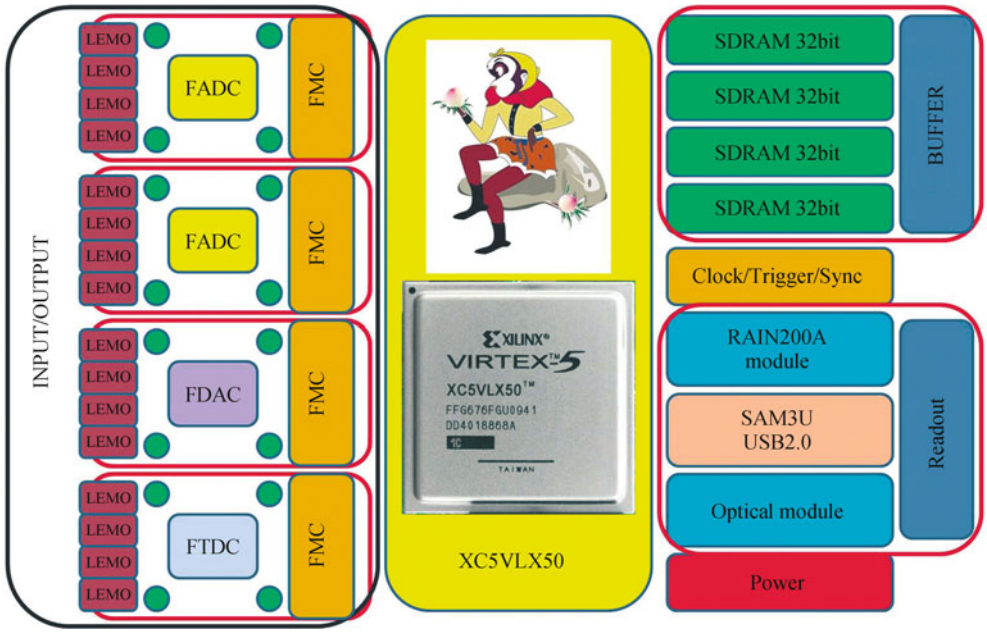

Fig. 20 The Wukong FADC/DAQ system for CDEX-1 and CDEX-10.

of the front-end fiber-optic interface of the back board.

- The Readout Electronics

  The CDEX electronic readout system is integrated on the Wukong board which is an electronic product developed by the researchers of Tsinghua University, and the module RAIN200A is used to read out the data of each Wukong Board. The module RAIN200A is based on PowerPC predecessor, where Linux2.6.X is running to obtain the readout data from FADC to Ethernet, with a bandwidth at least 95 Mbps.

  The RAIN200A has the following characteristics: The core predecessor is the 32-bit car-grade MPC5125 made by Freescale, with frequency of 400 MHz; the core board is installed with a 256 MB DDR2 industrial-grade memory and 4 GB NAND Flash; the core board is supplied with 100 Mbps Ethernet interface and USB 2.0 High-Speed interface; the system runs Linux 2.6.29 kernel with RT patch.

- DAQ

  The CDEX DAQ includes the electronic part acquiring data from the electronic units, the online data judgment, display and memory as well as the off-line data analysis etc.

  Because the electronic unit uses the Ethernet and TCP/IP as the interface of data readout, DAQ needs merely to acquire data for the standard protocol TCP/IP from the electronic unit, so that our scheme is very convenient. The architecture of the entire DAQ system is also an Ethernet-based exchange one and so the standard commercial switches, routers and Ethernet cards can be used to acquire data for the DAQ. Figure 20 gives the Wukong FADC/DAQ system for CDEX-1 and CDEX-10.

4 Detector performance

4.1 Physics requirement

As a detector used for DM detection, the most important requirement for it is its low background level. CDEX is to detect WIMPs with HPGe detectors, especially focusing on WIMPs of low masses (<10 GeV). This imposes another important requirement of energy threshold to the detector. The CDEX Collaboration adopts PCGe detectors for the low mass WIMP search which can realize a sub-keV energy threshold with kg-size mass. The ton-scale detector system of CDEX in the future will be realized based on this kind of kg-size PCGe detector. The PCGe detector has been developed from the conventional ULEGe detector. Many efforts have been contributed to optimize the application of the PCGe in DM searches.

- Pulse shape analysis of near noise-edge events extends the physics scope

  The PCGe detector can provide ULE down to

less than 500 eV. According to the theories on DM, the differential event rate of observing the recoiled nucleus scattered off by incident WIMPs exponentially increases with the decrease of its energy. So the pulse shape analysis of near noise-edge events is a very important task for the CDEX experiment to get lower energy threshold of the PCGe detector.

- Pulse shape analysis of surface versus bulk events to characterize an important background channel

  The location of an event where it is detected is another important parameter for background discrimination. For a PPCGe detector, due to the outside N^+ conjunction, there exists a thin layer which is called the "dead" layer. In fact, the thin layer is not really "dead", the events emerging in this thin layer can also give a different pulse shape from those bulk events which are produced in the interior part of the PPCGe detector. So the PSD methods should be developed for distinguishing the surface events from the bulk events.

- Sub-keV background clarification and suppression

  For the PCGe detector with a sub-keV energy threshold, it provides us a new energy window where so far no researches have ever covered this energy region due to relatively high energy threshold of those detectors. The CDEX experiment should first clarify the source and types of the background in the sub-keV energy region. Based on the present knowledge, a method for the background discrimination and suppression will be developed.

- Fabrication of advanced electronics for Ge detectors

  The PSD methods have been developed for suppressing noise, especially near the energy threshold, and discrimination of the surface events from bulk events. All these methods to obtain lower energy threshold and low background level are based on the performance of the front-end electronics of the PCGe detector. So another important requirement for the PCGe detector is the fabrication of advanced electronics for Ge detector which provides relatively low noise level.

4.2 Performance of CDEX-1

Since our first test run of 20 g-ULEGe in November of 2010, we have obtained some data during both commissioning period and formal data taking period. Data analysis is being undertaken for determining the final spectra, and the properties of the 20 g-ULEGe in this new CJPL environment have been known.

The Commissioning period data of 1 kg-PPCGe have also been acquired. The properties of this detector are shown in the following subsections.

4.2.1 Linearity calibration of 20 g-ULEGe and 1 kg-PPCGe

Because of the small volume of the detector, the detection efficiency of 20 g-ULEGe is relatively low in getting prominent peaks for calibration, even though the calibration period was prolonged to several months. Withal, there is no source available for further test in CJPL at present. An X-ray tube [61], which can generate X-ray of up to about 30 keV, is applied as a substitution of the source. When the X-ray generated by the tube hits the mixed powders of titanium dioxide (TiO_2) and potassium permanganate ($KMnO_4$), the characteristic X-rays can be used for the high gain (low energy range) calibration. The surrounding copper shielding contributes characteristic X-rays as well. Thanks to the thin carbon composite window of 0.6 mm, the overwhelming amount of the low energy X-rays are able to penetrate and deposit energies in the crystals. A sketch of the calibration for the 20 g-ULEGe is illustrated in Fig. 21.

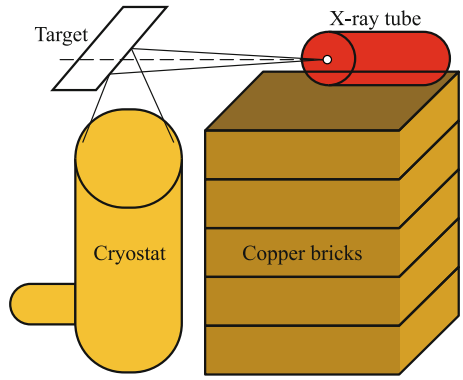

Fig. 21 Sketch of calibration for 20 g-ULEGe by X-ray tube.

The calibration result of the 20 g-ULEGe are shown in Fig. 22, with each sub-figure in accord with a 5 g sub-detector. In this scheme, characteristic X-rays of titanium, manganese and copper, coupled with random trigger [62] (zero point) are used (Table 1). From the fitting results of the seven points, we can observe a good linearity in the low energy range below 10 keV. Moreover, the region above 10 keV can be studied with available gamma sources.

Table 1 Sources for calibration of 20 g-ULEGe.

Source	Random trigger	Ti		Mn		Cu	
Energy/keV	0	4.509	4.932	5.895	6.490	8.041	8.904

The 1 kg-PPCGe does not have a carbon composite window, but a large volume and mass. So its detection efficiency is high enough to carry out a calibration with a few days' background data. The result of one data set is shown in Fig. 23, with 3 sub-figures corresponding to

Table 2 Sources for calibration of 1 kg-PPCGe.

High gain		Mediate gain		Low gain	
Source	Energy/keV	Source	Energy/keV	Source	Energy/keV
^{65}Zn	8.979	^{214}Pb	214.98	^{214}Pb	214.98
^{68}Ga	9.659	^{214}Pb	295.21	^{214}Pb	295.21
^{68}Ge	10.367	^{214}Pb	351.92	^{214}Pb	351.92
^{73,74}As	11.103	Ann	511.0	^{214}Bi	609.3
–	–	^{208}Tl	583.2	^{214}Bi	1120.3
–	–	^{214}Bi	609.3	^{214}Bi	1764.5
–	–	^{228}Ac	911.2	^{214}Bi	2204.2
–	–	^{214}Bi	1120.3	–	–

different gains. The period is 21.9 days and lots of background peaks are visible. Besides the zero point by random trigger, we use 4–8 points to complete the calibration fitting for different gains respectively (Table 2). The results also display a good linearity of the 1 kg-PPCGe.

4.2.2 Energy resolution of detectors 20 g-ULEGe and 1 kg-PPCGe

With the calibration data, the energy spectra as well as the properties of energy resolution have been obtained.

The calibrated spectra of the 20 g-ULEGe are plotted in Fig. 24. FWHM (fitted to a Gaussian function) are about 200 eV at 5 keV and about 300 eV at 9 keV. The 4 sub-detectors are very close to each other in all technical indices and practical performance. Besides the statistical limit, the X-ray tube which has a wide emission solid angel and notable energy dispersion also degenerate the

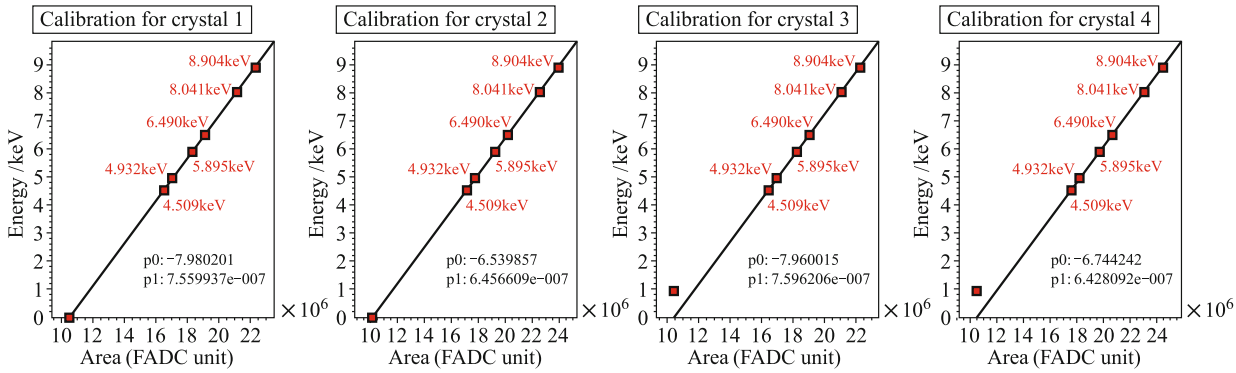

Fig. 22 Calibration result of 20 g-ULEGe.

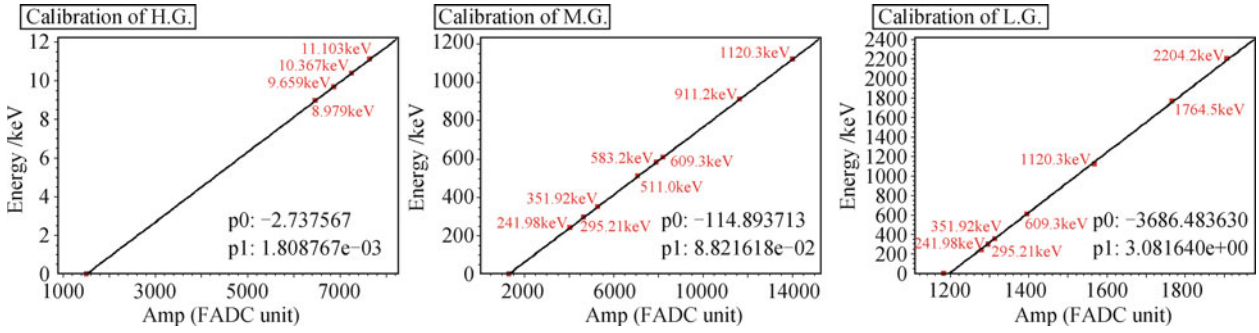

Fig. 23 Calibration result of 1 kg-PPCGe. *Left*: High gain. *Middle*: Mediate gain. *Right*: Low gain.

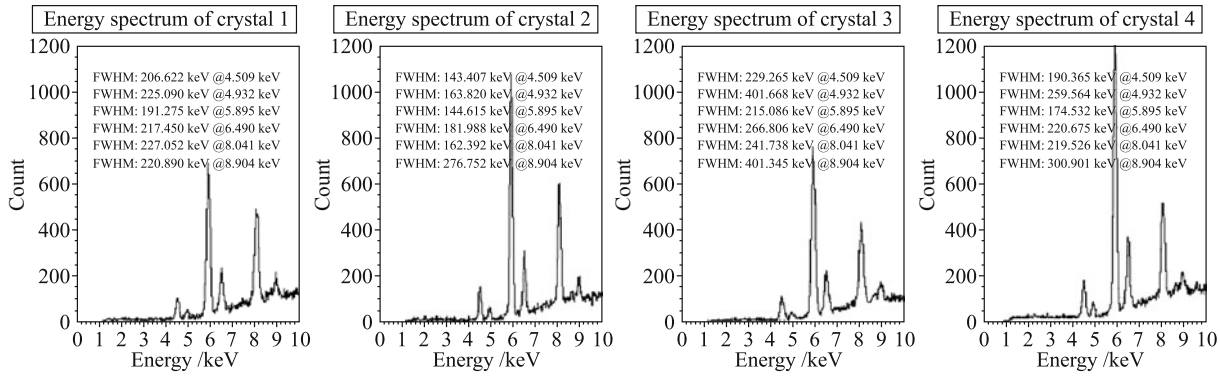

Fig. 24 Calibrated energy spectra of 20 g-ULEGe.

FWHM. So the energy resolution of the system is expected to be better than the predecessor products.

The calibrated spectra of 1 kg-PPCGe are plotted in Fig. 25. The FWHMs are about 200 eV at 10.367 keV and about 3.525 keV at 1120.3 keV. For many other peaks, FWHMs are limited by statistical errors, thus need to be improved with more data accumulation.

4.2.3 Noise level of 20 g-ULEGe and 1 kg-PPCGe

Electronic noise would crucially affect the energy threshold. To study the noise level, events by random trigger tag are selected and projected to energy spectra, which are then fitted with the Gaussian function. The FWHMs of the distributions render less than 100 eV of both 20 g-ULEGe (crystal 2) and 1 kg-PPCGe, which sustain the threshold lower than 500 eV (Figs. 26 and 27).

4.2.4 Stability of 20 g-ULEGe and 1kg-PPCGe

The validity of data which depict the system stability needs to be checked before overall data analysis. Several parameters describing the system behaviors are tracked over time, including the triggering rate, pedestal of pulse shape, noise level, etc. Figures 28 and 29 present the triggering rate status of 20 g-ULEGe and 1 kg-PPCGe, in which an average rate per hour is counted. Immoderate parts, especially an anomalous discrepancy deviating from the average level, should be carefully inspected and discarded if they are proved to be invalid.

4.2.5 Trigger efficiency

Trigger efficiency is to be checked before data analysis is carried on [46]. It determines the survival fractions of the events which pass the discriminator threshold. Specific pulse generator which can supply small signal ranged at 0–2 keV can be used to estimate the trigger efficiency at lower energy regions. Such a kind of pulse generatorsis under development right now, and the relevant test will be held soon.

5 Data analysis

5.1 Process

The data analysis is a very important step to understand the energy spectra of the HPGe detectors. Usually there are three sources contributing to the HPGe spectra: electronic noises and microphonic interference, physics background events as well as DM events. The purpose of the data analysis is first to discriminate out the noise, physics background events from the total energy spectra. Different methods need to be developed according to the characteristics of different sources.

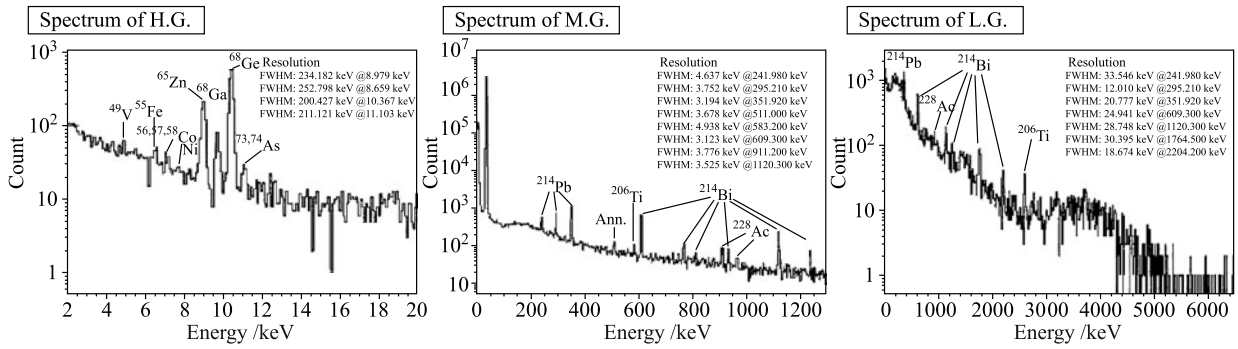

Fig. 25 Calibrated energy spectra of 1 kg-PPCGe. *Left*: High gain. *Middle*: Mediate gain. *Right*: Low gain.

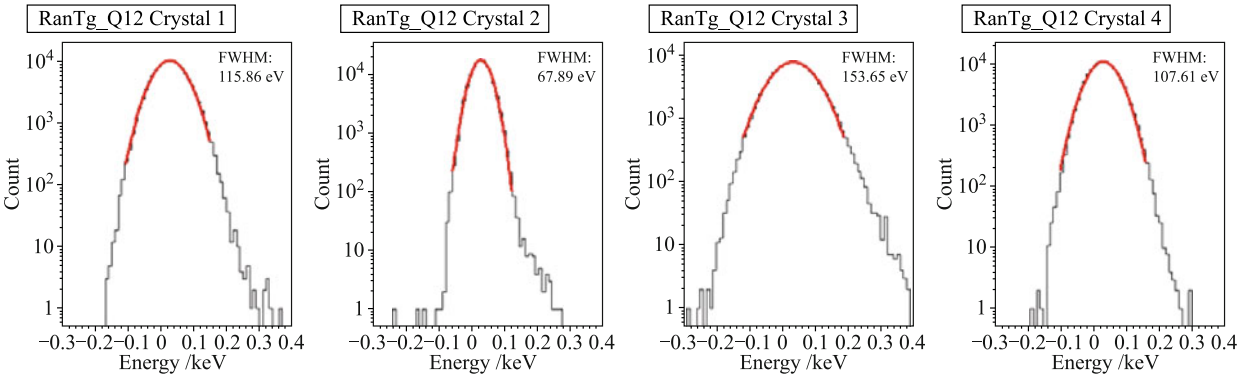

Fig. 26 Noise distribution of 20 g-ULEGe by random trigger.

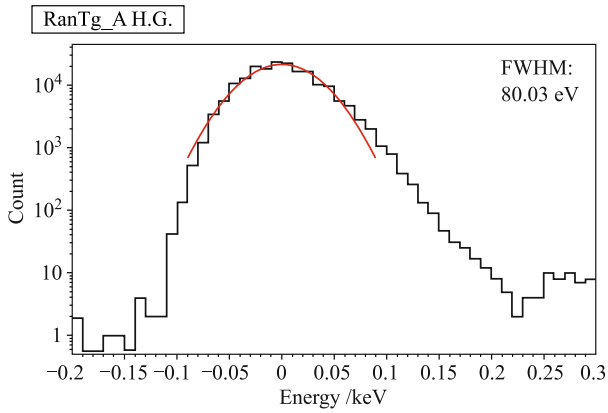

Fig. 27 Noise distribution of 1 kg-ULEGe by random trigger (high gain).

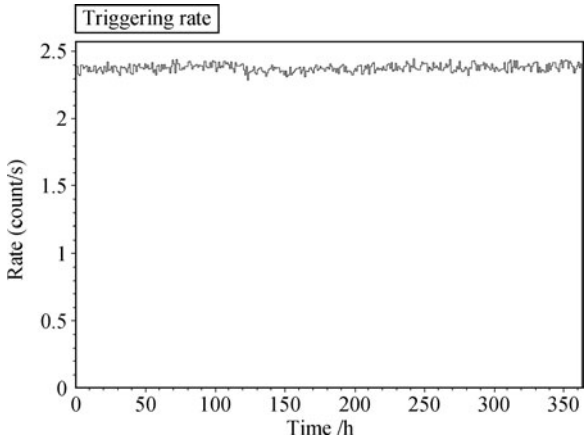

Fig. 28 Triggering rate status of 20 g-ULEGe.

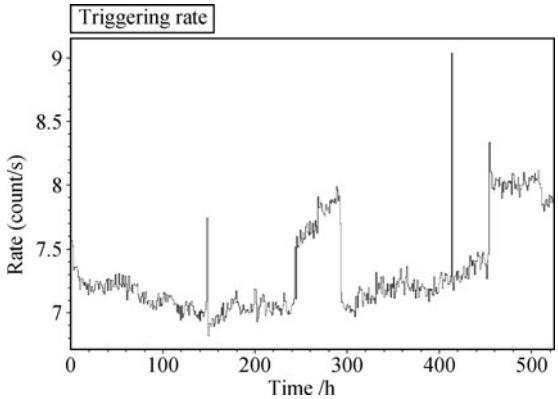

Fig. 29 Triggering rate status of 1 kg-PPCGe.

The signal shape of electronic noise and microphonic interference are not in the Gaussian-like wave form in which the WIMP events should be, then can be distinguished through some PSD method. Various parameters, time-to-peak, rise time and fall time, for instance, describing the wave form of the signal can be designed and used for differentiating in parameter plots. In contrast to the anomalous wave form, being analog to the Gaussian-like pulse shape would be a criterion for identifying the type of the sources in the calibration data. Take time-to-peak for instance. The shaping time of spectroscopy amplifier keeps constant, which results in almost the same rise time and fall time of different energy. Since HPGe trigger is produced by fixed discriminator (CAEN N844P) threshould, lower energy would have smaller pulse height, and thus the time difference between trigger and peak (defined as time-to-peak) is smaller. Such a relationship between time-to-peak and energy can be approximately fitted by a logarithmic function. So in the parameter plot of time-to-peak and energy, events far away from the logarithmic function would be discarded as noise events.

In particular, electronic noise exerts a crucial impact on the threshold and needs to be handled with great caution. Physics events (mainly background), in principle, follow the Gaussian distribution in 2D energy-energy parameter plot. So the threshold can be lower in this parameter plot than in a single energy spectrum plot. A noise edge cut, which exists along the tangent of the Gaussian distribution, is then set to lower the threshold. Since the cut is related to energy, the efficiency-energy curve should be estimated by the pulse calibration data or anti-Compton tagged data.

Usually in experiments of searching for DM one observes recoiled nuclei, such events might be tangled with the physics background caused by neutrons and electron recoil events. Several experiments, such as CDMS [63], XENON100 [64], CRESST-II [65], etc., used two distinct signals such as scintillation and ionization to reject the electron recoil events simultaneously. But it is not the case in CDEX, which only measures the energy deposition of ionization. So CDEX needs to consider only the quenching factor of energy deposit for the recoiled nucleus.

As the pulses caused by the electron recoil and nuclear recoil do not appear significantly different in the CDEX experiment , the normal PSD method would be less efficient here, some other aspects need to be viewed. There are mainly two ways to subtract the background events. One is to statistically eliminate the visible and invisible characteristic x-ray peaks; while the other is to apply some algorithm to reduce surface events occurring in the thin insensitive layer. In the low energy region which we are interested in, visible characteristic peaks usually come from the K-shell X-rays and the invisible ones are caused by the L-shell X-rays' contribution, both of which have been analyzed theoretically and experimentally in some details [66]. On the other hand, the surface insensitive layer of the PPCGe detector has a weaker electric field therefore can cause distortion of energy deposition. Such a kind of events would have slow pulse shape from preamplifier, but is degenerate with the electronic noise.

The Wavelet method [67] can reduce noise by filtering and shaping the signal sample.

With all the aforementioned processes, the final energy spectrum is obtained. Based on selected physics and statistical method, the final spectrum is then interpreted into physics result, namely the common exclusion curves.

5.2 Strategy

In order to measure the cross-sections for low WIMP masses, elaborate data analysis is essential to lower the threshold and single out background events from raw data. The threshold can be lowered by getting rid of noise events, and the non-WIMP event rate can be suppressed by deducting the microphonic events as well as physically identified non-WIMP events. Microphonic events, coming from violent changes of environment or instability of the system, usually have abnormal pulse shape. Non-WIMP events may consist of multi-site events, surface events (events with energy deposited in the dead layer of the surface), etc. To attain this goal, some variables or parameters are defined, either event by event or statistically. Figure 30 and Table 3 describe the notation of several empirical main parameters.

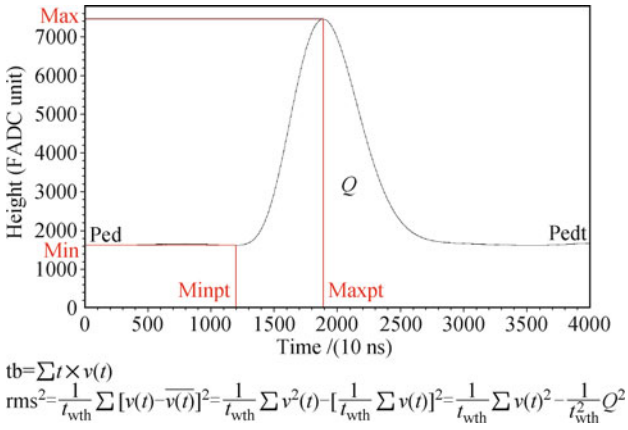

Fig. 30 Notation of several parameters.

Table 3 Definition of several parameters.

Notation	Description
Ped	Pedestal before the leading edge (head)
Pedt	Pedestal after the trailing edge (tail)
Max	Highest level
Maxpt	Highest time position
Min	Lowest level
Minpt	Lowest time position
Q	Total area (charge) of the full time window
Qp	Partial area (charge) of selected time window
tb	Time weighted integration
rms	Root mean square of the pulse shape

Some basic cuts for selection of pulse shapes, such as the stability of pedestal, time-to-peak, as well as linearity between area and amplitude, are applied firstly. After the pulse shape selection, three different crucial cuts are utilized as described in the following subsections. Then the derived final spectrum is used to interpret the physics, commonly by making exclusion plots or indicating islands in the parameter space.

Moreover, to identify the noise and microphonic events, reference pulse shape of physics signals are needed. Such physics signals can be selected within peaks of characteristic X-ray, either from calibration data or from background measurement.

5.2.1 *PSD cut*

Noise and microphonic events having different pulse shapes from the physics signals, can be distinguished through the PSD method. The parameters for each event pulse with different shaping time are then considered, and the scattered plot is shown in Fig. 31. The two parameters are the pulse amplitude with shaping times of 6 μs and 12 μs respectively. Red dots roughly along the diagonal stand for the physics and noise events, while the black dots in the band near the axes correspond to the interference events. So taking the straight lines (blue-colored) as cuts, we are able to discard the microphonic events. Determination of such straight lines is usually empirical, and efficiency correction has to be calculated thereafter.

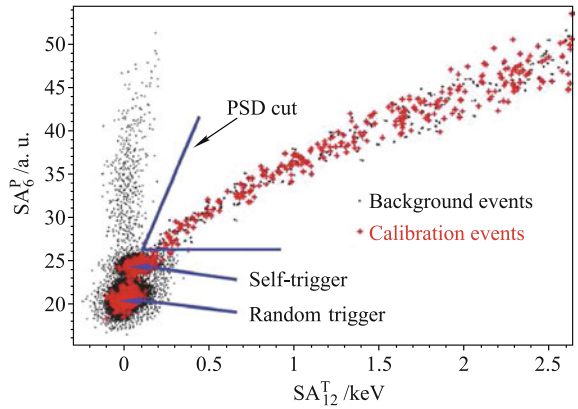

Fig. 31 Illustration of PSD cut [47].

5.2.2 *Noise edge cut*

In principle, the energy distribution of noise events is Gaussian. So in the 2D (such as calibrated Max and Q) parameter plot, the distribution seems like an ellipse truncated by discriminator threshold (Fig. 32). Whenever they are projected to either axis, the bulge would degrade the noise level. Noise edge cut is then used to reduce the noise events and hence lower the threshold. The straight line depends on both noise and signal dis-

tribution. The principle is to cut noise events as many as possible while leave signal events as many as possible. The key point is that since this cut is related to the energy, the efficiency curve has to be applied to make corrections. The efficiency curve is estimated by the pulse calibration data or anti-Compton tagged data, and the correction is calculated by dividing the efficiency for every energy bin. On this account, lower the threshold cannot guarantee better exclusion plot, because of the large uncertainty after efficiency correction.

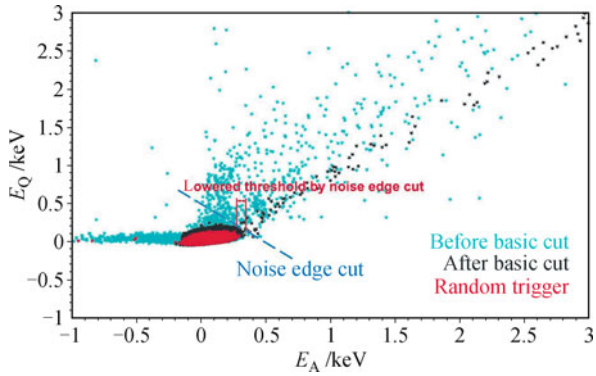

Fig. 32 Sketch of noise edge cut.

5.2.3 *Surface event cut*

Due to the manufacturing limitation, the N^+ contact surface layer of the PPCGe is thick (order of 1 mm), in which the electric field is weaker than in the crystal bulk so that the energy deposited in this layer cannot be efficiently collected. This layer is then named as the dead layer or insensitive layer, and the recorded events with energy deposited in this layer are called as surface events. The surface events have a longer charge-collection time and slower pulse shape, which may be kicked out by the time parameter cut. The rising time of the fast pulse at the preamplifier is chosen as the time parameter. However, in the low energy range which we are highly interested in, the signal-to-noise ratio becomes not high enough to finely deduce the parameter. The green curve in Fig. 33 shows a raw fast pulse. Marino [67] suggested a method that one can use a "wavelet" shrinkage to reduce noise. The result is shown as the black curve, and the rise time of 10%–90% of the leading edge is then estimated.

A typical tendency between the rising time and energy distribution is presented in Fig. 34, where two gatherings are clearly separated. The upper part which has longer rising time corresponds to the surface events, and then should be discarded by the red critical line. The lower part is then determined to be the final spectrum. Efficiency correction is needed afterwards, which could be estimated by source calibration data.

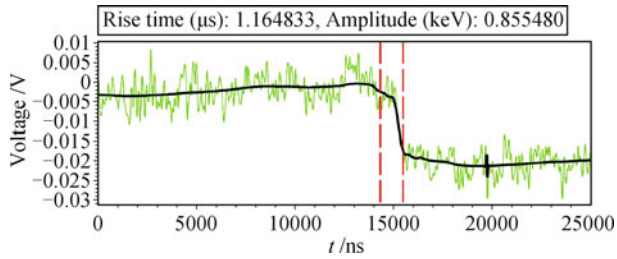

Fig. 33 Illustration of wavelet analysis [67].

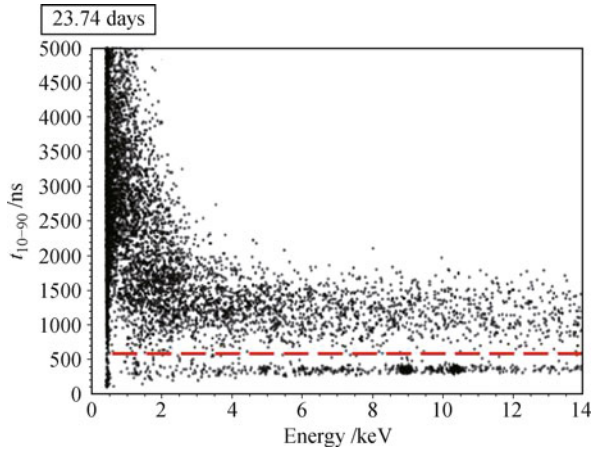

Fig. 34 Illustration of the surface event cut [68].

6 Prospect

6.1 Physical target

The CDEX Collaboration will carry out DM detection with PCGe arrays as the detector which is cooled down and actively shielded by the LAr system. The most interesting region for the CDEX experiment is the low WIMP mass region which could be detected by the ULE PCGe detector. Based on the performances of the prototype 1 kg-PPCGe detector which has run for several months in the shielding system at CJPL, the CDEX collaboration plans to focus on the direct detection of DM particles with a mass less than 10 GeV. The PCGe array system will run in CJPL and additional shielding system will be included such as 1 m thick PE for neutron deceleration and absorption, 20 cm lead and 20 cm OFHC copper for gamma shielding. An LAr cooling and active shielding system will be adopted for CDEX-10, and the PCGe detector will be immersed into the LAr system. The passive and active shielding systems provide the PCGe array system a relatively low background circumstance, thus running experiments with low background is expected. Except the shielding system, the effective PSD methods will also be developed to get rid of the noise and background events from the raw data and pick up the real DM events. These PSD methods mainly focus on (i) the pulse shape

analysis of the events near noise-edge to enlarge the observable physics range, (ii) the pulse shape analysis of surface events, by comparison with the bulk events that one can characterize the important background channel, (iii) understanding the sub-keV background and offering a scheme to suppress it.

By considering all possible effects in the design which might affect the performances of the detector and carrying careful dada analysis, we wish to achieve a level of 1 cpkkd (count per kilogram per keV per day) for both CDEX-1 and CDEX-10 stage. The different exclusive curves corresponding to different energy thresholds and background event rates are shown in Fig. 35.

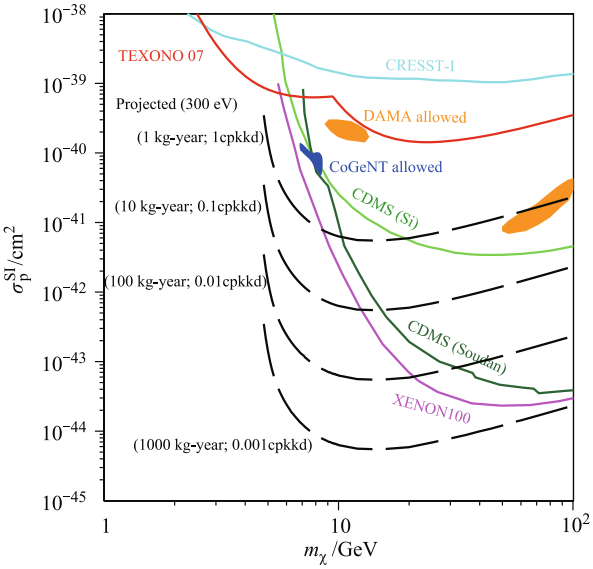

Fig. 35 The different exclusive curves corresponding to the different energy threshold and background event rate.

Improving the sensitivity of WIMP mass less than 10 GeV to 10^{-45} cm^2 is really a big challenge. It is indeed our goal. Right now our CDEX-1 data provides information about the background structure below 1 keV, which however cannot be identified for exposure limit. If the same background level exists for the CDEX-1T, we have confidence that we will be able to subtract more background to improve the sensitivity. Definitely lowering the threshold may also improve the sensitivity at low mass range. We agree that with all the available methods, a 4–5 order improvement is a rather tough goal.

6.2 CDEX-1T

The ultimate goal of the CDEX Collaboration is to set up a ton-scale mass Ge detectors based on the PCGe detector and LAr active shielding and cooling systems. The detailed design and technology which will be developed and utilized are based on the experience and lessons gained from the design and studies of the CDEX-10 detector. The detector will be located in a 1 m thick PE shielding room and the internal volume is covered by 20 cm lead and 10 cm OFHC copper. The threshold of less than 400 eV and background event rate of 0.001 cpkkd for the 1 ton Ge mass are the main goal of the CDEX-1T detector. The sensitivity for low mass DM will be down to about 10^{-45} cm^2 in the region of the WIMP mass less than 10 GeV if the 0.001 cpkkd background level is achieved, as shown in Fig. 35. The rough layout of the CDEX-1T detector is shown in Fig. 36.

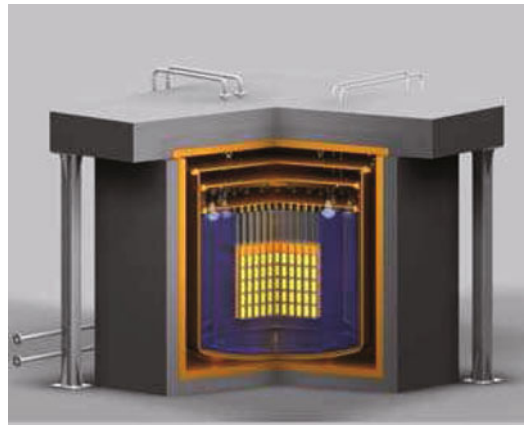

Fig. 36 Layout of the CDEX-1T detector system.

So far, upgrade of the CDEX detector system to O(1T) fiducial mass scale still remains at the conceptual stage. Much pre-research work has to be done step by step, just as the GERDA, XENON etc. collaborations are progressing. Right now we do not have a mature or concrete project how to design CDEX-1T. The only thing which is almost fixed is that CDEX-1T will inherit the design of PCGe crystal strings and LAr cooling & AC environment for the CDEX-10. The on-going CDEX-10 testing will provide us confidence about our design and the simulation and more knowledge and experience would be accumulated to modify the present design. Taking the LAr system as an example, we have to find if our current design is stable and able to be enlarged to at least 100 times. If not, we have to modify or change our project with other designs. Dividing 1000 1 kg-PCGe into several groups with individual LAr cooling and AC is another possible choice. By this sense, so far, we cannot offer more details about the CDEX-1T.

7 Summary

Astronomical observation, especially the CMB radiation and simulations for the large scale structure (LSS) of the universe indicate that a significant part of matter content of our universe is non-baryonic DM. The na-

ture of the DM is one of the fundamental problems of particle physics and cosmology. A favored candidate of DM is WIMPs. Direct searches of WIMPs are aiming at detecting the interaction of WIMPs with normal nuclei which are SM particles. The CDEX Collaboration is a new experimental group for searching DM in the world whose task is to directly search for WIMPs with ULE in terms of HPGe detector at CJPL. So far, the CDEX collaboration includes several members: Tsinghua university, Sichuan university, Nankai university, Institute of Atomic Energy, Yalong River Basin Company and Nuctech Company.

CJPL is located in the central portion of one of the transport tunnels of a giant hydrodynamic engineering project at the huge Jinping Mountain area of Sichuan province, southwest of China. The rock covering thickness of CJPL is about 2400 m where the cosmic muon flux is about 1 in 10^{-8} of the ground level. The muon flux, radioactivity and radon concentration in the underground lab have been measured and monitored time to time.

Comparing the detectors made of other materials the HPGe detector has many advantages such as low radioactivity, high energy resolution, high density and remarkable stability for radiation detection. CDEX adopts the PCGe with about 300 eV threshold to search for WIMPs of mass below 10 GeV. The detector mass of first phase CEDX-1 is 1 kg and that of second phase CDEX-10 is 10 kg.

There are two detectors of CDEX-1, 20 g-ULEGe and 1 kg-PPCGe, running now in CJPL. The detector is surrounded by CsI(Tl) or NaI(Tl) veto detector and outside the veto detector there is a shielding system. The performance of the detector has been calibrated, and the noise level is about 200 eV. The expectation of background count is less than 1 cpkkd near the 200 eV after event selection with the PSD cut, noise edge cut and wavelet cut.

CDEX-10 uses a PCGe detector array which is immersed into a LAr vessel. Each unit detector in the array is a 1 kg PCGe detector whose threshold is about 200 eV. The scintillation light in the LAr will be read out by the PMT, and the LAr is the cooling system providing working temperature for the Ge detector and also serves as a veto detector. The Monte Carlo study shows that the background event rate will be as low as 1 cpd at low energy range. In the future, the CDEX Collaboration is going to set up a ton-scale Ge detector composed of the PCGe detector and LAr active shielding and cooling system in CJPL. Hopefully, the overall threshold of the CDEX-1T detector will be less than 400 eV and the background event rate could be reduced to 0.001 cpd. The sensitivity will be down to about 10^{-45} cm^2 for a WIMP mass as low as 10 GeV or even less.

Acknowledgements This work was partly supported by the National Natural Science Foundation of China (NNSFC), Ministry of Science and Technology of China (MOSTC), and Ministry of Education of China.

References and notes

1. F. Zwicky, On the masses of nebulae and of clusters of nebulae, *Astrophys. J.*, 1937, 86: 217
2. V. Rubin and W. K. J. Ford, Rotation of the andromeda nebula from a spectroscopic survey of emission regions, *Astrophys. J.*, 1970, 159: 379
3. V. Rubin, W. K. J. Ford, and N. Thonnard, Rotational properties of 21 SC galaxies with a large range of luminosities and radii, from NGC 4605 /R = 4 kpc/ to UGC 2885 /R = 122 kpc/, *Astrophys. J.*, 1980, 238: 471
4. V. Rubin, D. Burstein, W. K. J. Ford, and N. Thonnard, Rotation velocities of 16 SA galaxies and a comparison of Sa, Sb, and SC rotation properties, *Astrophys. J.*, 1985, 289: 81
5. D. Clowe, M. Bradac, A. H. Gonzalez, M. Markevitch, S. W. Randall, C. Jones, and D. Zaritsky, A direct empirical proof of the existence of dark matter, *Astrophys. J.*, 2006, 648(2): L109
6. J. Beringer, et al. [Particle Data Group], The review of particle physics, *Phys. Rev. D*, 2012, 86: 010001
7. Planck Collaboration, Planck 2013 results. XVI. cosmological parameters, arXiv: 1303.5076v1, 2013
8. V. Trimble, Existence and nature of dark matter in the universe, *Annu. Rev. Astron. Astrophys.*, 1987, 25(1): 425
9. G. Jungman, M. Kamionkowski, and K. Griest, Supersymmetric dark matter, *Phys. Rep.*, 1996, 267(5–6): 195
10. L. Bergstrom, Dark matter candidates, *New J. Phys.*, 2009, 11(10): 105006
11. J. L. Feng, Dark matter candidates from particle physics and methods of detection, arXiv: 1003.0904, 2010
12. R. J. Gaitskell, Direct detection of dark matter, *Ann. Rev. Nucl. Part. Sci.*, 2004, 54(1): 315
13. X. G. He, H. C. Tsai, T. Li, and X. Q. Li, Scalar dark matter effects in Higgs and top quark decays, *Mod. Phys. Lett. A*, 2007, 22(25n28): 2121
14. X. He, T. Li, X. Q. Li, J. Tandean, and H. C. Tsai, Constraints on scalar dark matter from direct experimental searches, *Phys. Rev. D*, 2009, 79(2): 023521
15. A. Beylyaev, M. T. Frandsen, S. Sarkar, and F. Sannino, Mixed dark matter from Technicolor, *Phys. Rev. D*, 2011, 83(1): 015007, and the references therein
16. H. P. An, S. L. Chen, R. N. Mohapatra, S. Nussinov, and Y. Zhang, Energy dependence of direct detection cross-section for asymmetric mirror dark matter, *Phys. Rev. D*, 2010, 82: 023533, arXiv: 1004.3296
17. J.-W. Cui, H.-J. He, L.-C. Lu, and F.-R. Yin, Spontaneous mirror parity violation, common origin of matter and dark

matter, and the LHC Signatures, *Phys. Rev. D*, 2012, 85: 096003, arXiv: 1110.6893

18. M. Gilloz, A. von Manteuffel, P. Schwaller, and D. Wyler, The little skyrmion: new dark matter for little Higgs models, *J. High Energy Phys.*, 2011, 1103: 48, and references therein, arXiv: 1012.5288v2
19. J. Lavalle, J. M. Alimi, and A. Fuözfa, Cosmic ray positron excess: Is the dark matter solution a good bet? *AIP Conf. Proc.*, 2010, 24: 398
20. R. Yang, J. Chang, and J. Wu, A possible explanation for the electron/positron excess of ATIC/PAMELA, *Res. Astro. Astrophys.*, 2010, 10(1): 39, and references therein
21. M. Amenomori, et al. [Tibet AS-gamma Collaboration], Cosmic-ray energy spectrum around the knee observed with the Tibet air-shower experiment, *Astrophys. Space Sci. Trans.*, 2011, 7(1): 15
22. M. Aguilar, et al. [AMS Collaboration], First result from the alpha magnetic spectrometer on the international space station: Precision measurement of the positron fraction in primary cosmic rays of 0.5–350 GeV, *Phys. Rev. Lett.*, 2013, 110(14): 141102
23. K. Bernabei, P. Belli, F. Cappella, R. Cerulli, C. J. Dai, A. d'Angelo, H. L. He, A. Incicchitti, H. H. Kuang, J. M. Ma, F. Montecchia, F. Nozzoli, D. Prosperi, X. D. Sheng, and Z. P. Ye, First results from DAMA/LIBRA and the combined results with DAMA/NaI, *Eur. Phys. J. C*, 2008, 56(3): 333
24. K. Bernabei, P. Belli, F. Cappella, R. Cerulli, C. J. Dai, A. d'Angelo, H. L. He, A. Incicchitti, H. H. Kuang, X. H. Ma, F. Montecchia, F. Nozzoli, D. Prosperi, X. D. Sheng, R. G. Wang, and Z. P. Ye, New results from DAMA/LIBRA, *Eur. Phys. J. C*, 2010, 67(1–2): 39
25. C. Aalseth, P. S. Barbeau, N. S. Bowden, B. Cabrera-Palmer, et al., Results from a search for light-mass dark matter with a *p*-type point contact germanium detector, *Phys. Rev. Lett.*, 2011, 106(13): 131301
26. P. Brink, Z. Ahmed, D. S. Akerib, C. N. Bailey, et al., The cryogenic dark matter search (CDMS): Present status and future, *AIP Conf. Proc.*, 2009, 1182: 260
27. G. Angloher, et al. [CRESST Collaboration], Results from 730 kg days of the CRESST-II dark matter search, arXiv: 1109.0702, 2011
28. J. Angle, et al. [XENON10 Collaboration], Search for light dark matter in XENON10 data, *Phys. Rev. Lett.*, 2011, 107: 051301
29. R. Agnese, et al. [CDMS Collaboration], Dark matter search results using the silicon detectors of CDMS II, arXiv: 1304.4279v2, 2013
30. M. T. Frandsen, F. Kahlhoefer, C. McCabe, S. Sarkar, and K. Schmidt-Hoberg, The unbearable lightness of being: CDMS versus XENON, arXiv: 1304.6066v1, 2013
31. X. G. He and J. Tandean, Low-mass dark-matter hint from CDMS II, Higgs boson at LHC, and Darkon models, arXiv: 1304.6058v1, 2013
32. E. Aprile, et al. [XENON100 Collaboration], Dark matter results from 225 live days of XENON100 data, arXiv: 1207.5988v2, 2013
33. J. Angle, et al. [XENON Collaboration], Limits on spin-dependent WIMP-nucleon cross-sections from the XENON10 experiment, *Phys. Rev. Lett.*, 2008, 101(9): 091301
34. M. T. Ressell, M. Aufderheide, S. Bloom, K. Griest, G. Mathews, and D. Resler, Nuclear shell model calculations of neutralino-nucleus cross-sections for ^{29}Si and ^{73}Ge, *Phys. Rev. D*, 1993, 48(12): 5519
35. G. Griest, Cross-sections, relic abundance, and detection rates for neutralino dark matter, *Phys. Rev. D*, 1988, 15(8): 2357
36. C. L. Shan, Effects of residue background events in direct dark matter detection experiments on the estimation of the spin-independent WIMP-nucleon coupling, arXiv: 1103.4049v2, 2011
37. C. L. Shan, Estimating the spin-independent WIMP-nucleon coupling from direct dark matter detection data, arXiv: 1103.0481v2, 2011
38. V. Barger, W.-Y. Keung, and G. Shaughnessy, Spin dependence of dark matter scattering, *Phys. Rev. D*, 2008, 78: 056007, arXiv: 0806.1962
39. Y. Tzeng and T. T. S. Kuo, Dark matter-nucleus scattering, 14th International Conference on Particles and Nuclei (PANIC 96): C96-05-22, 479
40. M. T. Ressell, M. Aufderheide, S. Bloom, K. Griest, G. Mathews, and D. Resler, Nuclear shell model calculations of neutralino-nucleus cross-sections for ^{29}Si and ^{73}Ge, *Phys. Rev. D*, 1993, 48(12): 5519
41. M. T. Ressell and D. J. Dean, Spin-dependent neutralino-nucleus scattering for A127 nuclei, *Phys. Rev. C*, 1997, 56(1): 535
42. J. Engel, S. Pittel, and P. Vogel, Nuclear physics of dark matter detection, *Int. J. Mod. Phys. E*, 1992, 1: 1
43. J. Engel, Nuclear form factors for the scattering of weakly interacting massive particles, *Phys. Lett. B*, 1991, 264(1–2): 114
44. Q. Yue, J. P. Cheng, Y. J. Li, J. Li, and Z. J. Wang, Detection of WIMPs using low threshold HPGe detector, *High Energy Physics and Nuclear Physics*, 2004, 28(8): 877 (in Chinese)
45. X. Li, Q. Yue, Y. J. Li, J. Li, et al., Status of ULE-HPGe detector experiment for dark matter search, *High Energy Physics and Nuclear Physics*, 2007, 31(6): 564 (in Chinese)
46. S. T. Lin, et al. [TEXONO Collaboration], New limits on spin-independent and spin-dependent couplings of low-mass WIMP dark matter with a germanium detector at a threshold of 220 eV, *Phys. Rev. D*, 2009, 79(6): 061101(R)
47. C. E. Aalseth, et al. [CoGeNT Collaboration], Results from a search for light-mass dark matter with a *p*-type point contact germanium detector, *Phys. Rev. Lett.*, 2011, 106(13): 131301
48. C. E. Aalseth, et al. [CoGeNT Collaboration], Search for an annual modulation in a *p*-type point contact germa-

nium dark matter detector, *Phys. Rev. Lett.*, 2011, 107(14): 141301

49. Majorana Collaboration, http://www.npl.washington.edu/majorana/
50. GERDA Collaboration, http://www.mpi-hd.mpg.de/gerda/
51. K. J. Kang, J. P. Cheng, Y. H. Chen, Y. J. Li, M. B. Shen, S. Y. Wu, and Q. Yue, Status and prospects of a deep underground laboratory in China, *J. Phys.: Conf. Ser.*, 2010, 203(1): 012028
52. D. Normile, Chinese scientists hope to make deepest, darkest dreams come true, *Science*, 2009, 324(5932): 1246
53. G. Heusser, Low-radioactivity background techniques, *Ann. Rev. Nucl. Part. Sci.*, 1995, 45(1): 543
54. Canberra, http://www.canberra.com/
55. Chinalco Luoyang Copper Co, Ltd, http://www.lycopper.cn
56. ORTEC, http://www.ortec-online.com
57. Y. C. Wu, et al. [CDEX Collaboration], Measurement of cosmic ray flux in China Jinping underground laboratory, arXiv: 1305.0899, 2013
58. Saphymo, http://saphymo.de
59. P. N. Luke, F. S. Goulding, N. W. Madden, and R. H. Pehl, Low capacitance large volume shaped-field germanium detector, *IEEE Trans. Nucl. Sci.*, 1989, 36(1): 926
60. P. S. Barbeau, J. I. Collar, and O. Tench, Large-mass ultralow noise germanium detectors: performance and applications in neutrino and astroparticle physics, *J. Cosmol. Astropart. Phys.*, 2007, 09: 009
61. AMPTEK, http://www.amptek.com
62. TEK, http://www.tek.com
63. CDMS Collaboration, http://cdms.berkeley.edu
64. XENON Collaboration, http://xenon.astro.columbia.edu
65. CRESST Collaboration, http://www.cresst.de
66. C. Aalseth, P. S. Barbeau, J. Colaresi, J. I. Collar, et al., Search for an annual modulation in a p-type point contact germanium dark matter detector, *Phys. Rev. Lett.*, 2011, 107(14): 141301
67. M. G. Marino, Dark matter physics with P-type point-contact germanium detectors: Extending the physics reach of the Majorana experiment, Ph.D. Dissertation, University of Washington, 2010
68. From a talk given by J. F. Wilkerson in Tsinghua University in 2011